Texas Coastal Nutrient Input Repository – Phase 1 Lavaca Bay

Final Report

GLO Contract No. 22-045-009-D106

March 2023

Michael Schramm, Research Specialist III

Texas A&M AgriLife Research
Texas Water Resources Institute
1001 Holleman Dr. E.
College Station, TX 77840-2118

Submitted to:
Texas General Land Office
1700 Congress Ave.
Austin, TX 78701-1495

This report was funded in part by a Texas Coastal Management Program grant approved by the Texas Land Commissioner, providing financial assistance under the Coastal Zone Management Act of 1972, as amended, awarded by the National Oceanic and Atmospheric Administration (NOAA), Office for Coastal Management, pursuant to NOAA Award No. NA21NOS4190136. The views expressed herein are those of the author(s) and do not necessarily reflect the views of NOAA, the U.S. Department of Commerce, or any of their subagencies.

Summary

Recent studies have identified an increasing number of areas along the Texas coastline with water quality conditions conducive to algal blooms and eutrophication. These conditions are driven by changes in land use, population, water diversions, and effluent discharges in upstream watersheds that lead to degraded water quality in downstream estuaries. This study explored the both the use of semiparametric statistical models to quantify nutrient loadings within the Lavaca Bay watershed and the linkages between watershed loadings and downstream water quality.

Results indicate that the statistical modeling approaches performed well at predicting loads, although additional flow-biased data collection efforts would be useful for assessing performance under critical high-flow loading events. The study also found that variation in nutrient loading within the Lavaca Bay watershed is driven primarily by changes watershed runoff and streamflow, not by changes in nonpoint sources. When modeling the linkages between Lavaca Bay water quality and watershed runoff and loading, strong links were identified between flows and nutrient concentrations in the Bay. However, we found little evidence of positive or negative effects of flows on dissolved oxygen within the Bay. In contrast, the study did find linkages between flow-adjusted loads and Total Phosphorus (TP) concentration in the Bay but did not identify a link between Nitrate (NO_3) loads and Nitrite+Nitrate (NO_x) concentrations. This study lacked sufficient data to develop load estimates of total nitrogen or total Kjeldahl nitrogen which may provide more information than Nitrate when it comes to Lavaca Bay water quality.

Nutrient Load Models

NO_3 and TP load models were developed for the Lavaca River at USGS Stream Gage 08164000, and the Navidad River at the discharge of Lake Texana at approximately at USGS-08164525. Additional loading models were developed at sites upstream of Lake Texana at the Navidad River, Sandy Creek, West Mustang Creek, and East Mustang Creek. A site map is included in the main text report below. A semiparametric model approach was utilized to develop non-linear

relationships between nutrient concentrations and time, discharge, season, and antecedent discharge. Daily loads were then determined by multiplying predicted concentrations and measured mean daily streamflow. Model assessments indicated that the approach performed well for predicting daily loading at most sites. The approach and results are explained further in this report and the following technical report:

Schramm, M. 2023. Texas Coastal Nutrient Input Repository - Task 4 Report Statistical Models for Nutrient Loading into Lavaca Bay. College Station, TX: Texas Water Resources Institute. TR-543. https://twri.tamu.edu/publications/technical-reports/2023-technical-reports/tr-543/.

Data Repository

The R code used to develop models and predict daily loads, and the final model predictions are available in the Zenodo data repository, https://doi.org/10.5281/zenodo.7330754. The project can also be accessed via the TWRI GitHub page to facilitate project cloning and reproduction using the appropriate R software packages: https://github.com/TxWRI/lavaca-nutrients. Finally, nutrient load data can be directly downloaded with documented metadata at: https://txwri.github.io/lavaca-nutrients/. Presentations, data, code, and reports generated by this project are currently available on a project website (https://tcnir.twri.tamu.edu/). A public-facing data dashboard on the project webpage provides visual representations of site locations and load estimates generated by our models in downloadable text delimited files (Figure 1).

Data Analysis

The study utilized predicted nutrient loads to evaluate temporal trends, and the effect of freshwater inflow and nutrient loading and water quality components at three long-term monitoring sites in Lavaca Bay. Results are detailed in the main body of this final report and the following technical report:

Schramm, M. 2023. Texas Coastal Nutrient Input Repository – Task 3 Report Lavaca Bay Water Quality Responses to Nutrient Loading. College Station, TX: Texas Water Resources Institute. TR-546. https://twri.tamu.edu/publications/technical-reports/2023-technical-reports/tr-546/.

Engagement

An advisory committee of local stakeholders was formed for the project to discuss results and usefulness of the data. The committee held two meetings and was composed of the following individuals:

- Chad Kinsfather – Lavaca Navidad River Authority
- Bill Balboa – Matagorda Bay Foundation
- Brian Koch – Texas State Soil and Water Conservation Board
- Janet Weaver – Lavaca Bay Foundation
- Mike Wetz – Texas A&M University, Corpus Christi
- Jason Pinchback – Texas General Land Office
- RJ Shelly – Texas Sea Grant

Project results were presented during the water quality session of the American Water Resources Association National Conference in Seattle, WA (November 2022). A manuscript has also been submitted for peer review:

Schramm, M. Assessing linkages between watershed nutrient loading and water quality in a subtropical estuary with semiparametric models. *(submitted).*

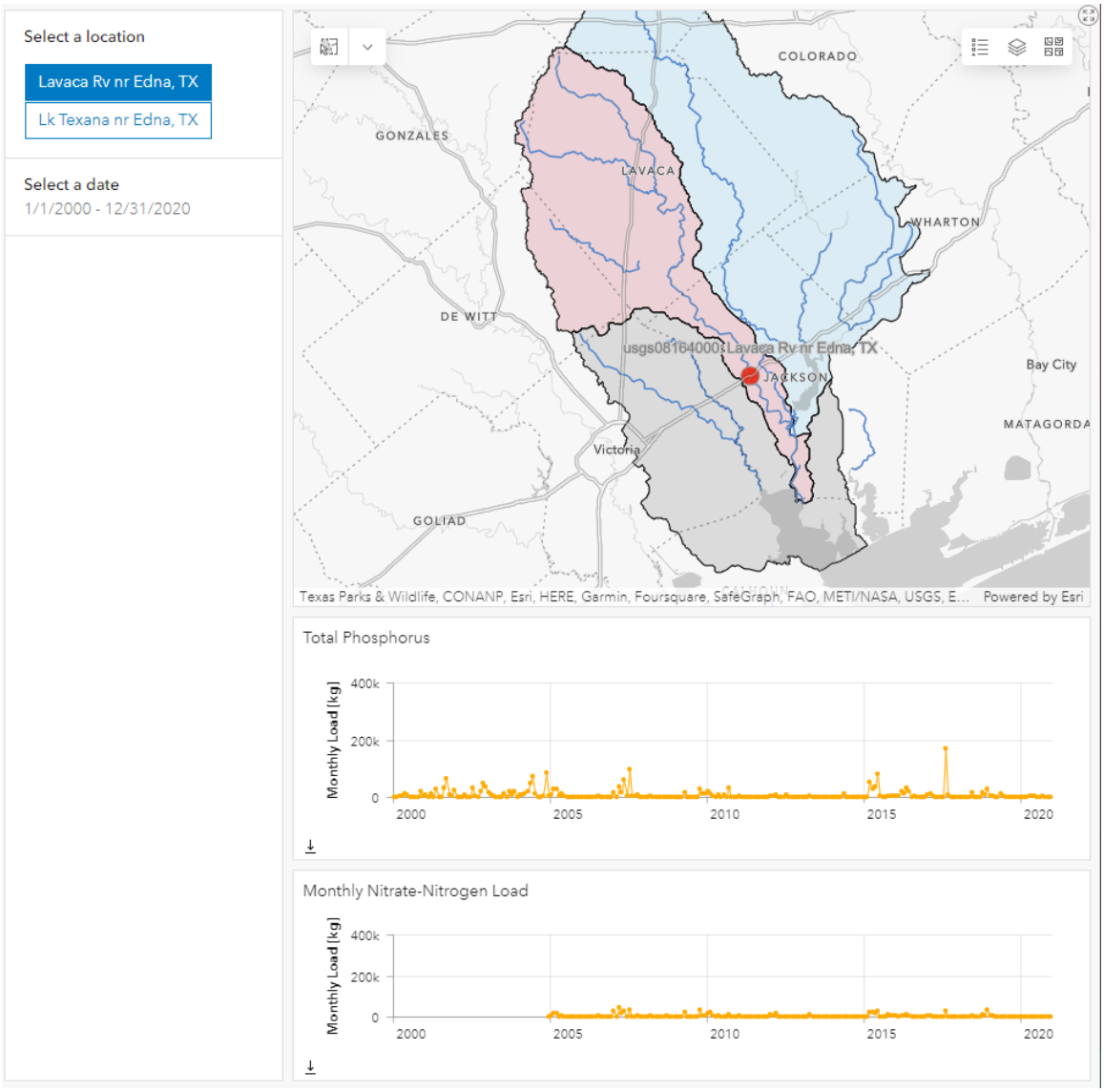

Figure 1. ArcGIS dashboard and data viewer.

Contents

Figure

Tables

Introduction

Like many coastal areas globally, the coastal watersheds along the Texas Gulf coast are facing pressures from increasing population, increases in point source and non-point source pollution and alterations to freshwater flows that degrade water quality in downstream estuaries (Bricker et al. 2008; Kennicutt 2017; Bugica et al. 2020). Despite escalating pressures, national scale assessments have classified coastal estuaries in Texas as moderate or low risk for eutrophic conditions (Bricker et al. 2008). However, a suite of recent studies indicates that estuary water quality dynamics in both agriculturally dominated and urban watersheds within Texas are in fact expressing conditions that are increasingly conducive to algal blooms and eutrophication (Wetz et al. 2016; Wetz et al. 2017; Bugica et al. 2020; Chin et al. 2022). With identification of localized areas of estuary water quality concern along the Texas coast (Bugica et al. 2020), localized studies are being prioritized to better inform management actions.

This project provides an assessment of nutrient loading and water quality responses in Lavaca Bay, Texas. Lavaca Bay is a secondary bay in the larger Matagorda Bay system located roughly halfway between Houston, Texas and Corpus Christi, Texas. Lavaca Bay faces substantial challenges associated with legacy contamination, but general water quality parameters such as dissolved oxygen (DO), nutrients, and biological parameters have been well within state water quality standards. However, long-term declines of benthic fauna abundance, biomass, and diversity in Lavaca Bay primarily linked to reductions in freshwater inflows and changes in estuary salinity are a concern to local stakeholders (Beseres Pollack et al. 2011; Palmer and Montagna 2015; Montagna et al. 2020). Recent water quality assessments identified monotonic increases in Total Phosphorus (TP), orthophosphate, total Kjeldahl nitrogen (TKN), and chlorophyll-*a* at sites within Lavaca Bay (Bugica et al. 2020). Although long-term changes in DO

concentrations were not identified, the trends in nutrient concentrations are concerning due to the role of nitrogen as a limiting factor for primary production in many Texas estuaries (Gardner et al. 2006; Hou et al. 2012; Dorado et al. 2015; Wetz et al. 2017; Paudel et al. 2019) and the ramifications that changes in nitrogen loadings could have for productivity and eutrophication in Lavaca Bay.

There are ongoing efforts between local, state, and federal agencies to address water quality impairments in the freshwater portions of the Lavaca Bay watershed (Schramm et al. 2018; Berthold et al. 2021; Jain and Schramm 2021). However, at a statewide scale, these approaches have shown limited success and emphasize a need for improved efforts at assessing and linking management actions with downstream water quality to identify and replicate effective management actions across the state (Schramm et al. 2022). The identification and communication of changes and trends in water quality is complicated by the fact that trends are often non-linear and confounded by precipitation and runoff that hinder traditional analysis (Wazniak et al. 2007; Lloyd et al. 2014). To provide actionable information for resource managers, water quality conditions must be evaluated relative to changes in natural environmental drivers to better understand and manage potential anthropogenic effects. This study utilizes semiparametric methods to develop estimates of delivered and flow-normalized nutrient loads and assess changes in loads delivered to Lavaca Bay. The study also assesses the response of water quality parameters in Lavaca Bay over time and in response to freshwater inflow controlled for seasonality and to watershed nutrient loads that are controlled for environmentally driven variation.

Materials and Methods

Study Area and Data

Lavaca Bay is 190 km^2 with the majority of freshwater inflow provided by the Lavaca and Navidad River systems (Figure 2). The Garcitas-Arenosa, Placedo Creek, and Cox Bay

watersheds provide additional freshwater inflows. The entire watershed land area is 8,149 km^2 and primarily rural. Watershed land cover and land use is 50% grazed pasture and rangeland, 20% cultivated cropland (primarily row crops such as corn, cotton, and sorghum), and 5% suburban/urban. Pasture and rangeland are concentrated in the Lavaca River watershed, while cultivated crops are generally located along the eastern tributaries of the Navidad river. The Lavaca and Navidad River watersheds are a combined 5,966 km^2, or approximately 73% of the entire Lavaca Bay watershed area. Discharge from the Navidad River is regulated by Lake Texana which has been in operation since 1980. Lake Texana provides 0.210 km^3 of water storage and discharges into the tidal section of the Navidad River which ultimately joins the tidal section of the Lavaca River 15 km upstream of the confluence with the Lavaca Bay.

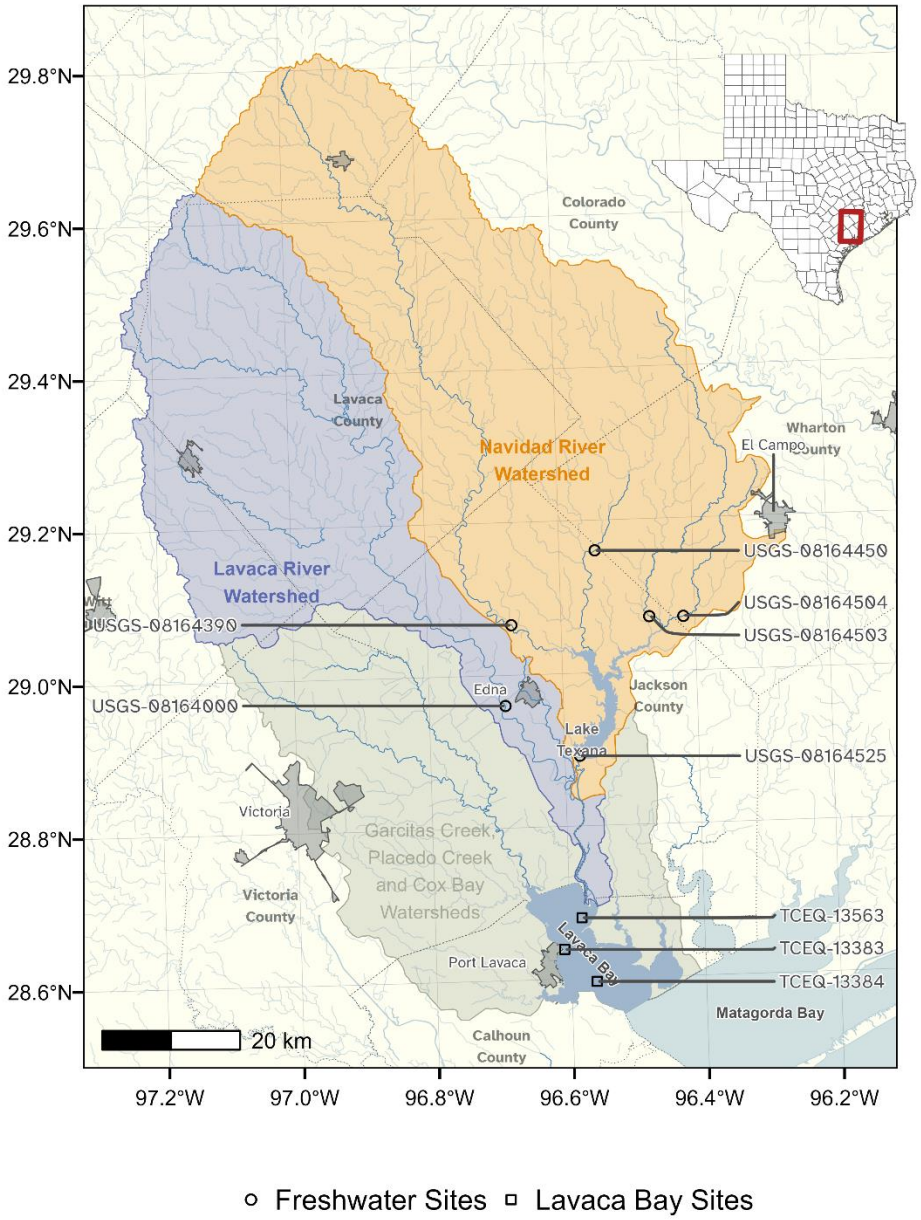

Figure 2. Lavaca Bay watersheds and site locations used for modeling nutrient loads and estuary water quality responses.

Daily discharges for the Lavaca River (USGS-08164000, Fig 1) were obtained from the United States Geologic Survey (USGS) National Water Information System using the *dataRetrieval* R package (De Cicco et al. 2022). Gaged daily discharges from the outlet of

Lake Texana on the Navidad River (USGS-0816425) were provided by the Texas Water Development Board (TWDB) (April 21, 2022 email from R. Neupane, TWDB).

Water quality sample data for the two freshwater and three estuary locations were obtained from the Texas Commission on Environmental Quality (TCEQ) Surface Water Quality Monitoring Information System. Data submitted through the system are required to be collected under Quality Assurance Project Plans (QAPPs) and lab method procedures outlined by the TCEQ's procedures manual. The QAPP and procedures manuals ensure consistent collection and laboratory methods are applied between samples collected by different entities and under different projects. All sites had varying lengths of and availability of data. For freshwater locations, TP from January 2000 through December 2020 and nitrate-nitrogen (NO_3) data from January 2005 through December 2020 were downloaded (Table 1). Less than 5-years of quarterly total nitrogen and TKN concentration data were available at the freshwater sites and deemed insufficient to develop load estimation models (Horowitz 2003; Snelder et al. 2017). The three estuary sites included an upper Lavaca Bay site near the outlet of the Lavaca River system (TCEQ-13563), a mid-Lavaca Bay site (TCEQ-13383), and the lower Lavaca Bay site near the mouth of the Bay (TCEQ-13384). For estuary locations, we obtained data for TP, Nitrite+Nitrate (NO_x), TKN, chlorophyll-*a*, and DO concentrations from January 2005 through December 2020 (Table 2).

Table 1. Summary of mean daily discharge, NO_3, and TP at freshwater sites between January 1, 2000, and December 31, 2020

		Mean Daily Discharge (cfs)		NO_3 (mg/L)		TP (mg/L)	
Site	**Description**	**Mean (SD)**	**N**	**Mean (SD)**	**N**	**Mean (SD)**	**N**
USGS-08164000	Lavaca River near Edna	332.78 (1667.47)	7,671	0.18 (0.24)	74	0.21 (0.09)	80
USGS-08164390	Navidad River at Strane Pk.	222.83 (926.18)	7,671	0.17 (0.15)	59	0.21 (0.09)	77
USGS-08164450	Sandy Creek near Ganado	176.63 (730.01)	7,671	0.17 (0.17)	56	0.21 (0.20)	75
USGS-08164503	West Mustang Creek near Ganado	144.65 (617.38)	7,671	0.45 (0.57)	63	0.32 (0.23)	81
USGS-08164504	East Mustang Creek near Lousie	39.58 (202.06)	7,671	1.15 (2.52)	61	0.40 (0.31)	79
USGS-08164525	Lake Texana (Navidad River)	666.14 (2957.79)	7,671	0.29 (0.26)	62	0.20 (0.08)	81

Table 2. Summary of estuary water quality samples collected between January 1, 2005, and December 31, 2020.

Station ID	Parameter	Mean	SD	N
TCEQ-13383	TP (mg/L)	0.11	0.05	47
	NO_x (mg/L)	0.07	0.15	51
	TKN (mg/L)	0.94	0.49	45
	Chlorophyll-*a* (µg/L)	9.43	5.31	47
	DO (mg/L)	7.22	1.35	55
TCEQ-13384	TP (mg/L)	0.08	0.03	51
	NO_x (mg/L)	0.06	0.08	52
	TKN (mg/L)	0.76	0.40	48
	Chlorophyll-*a* (µg/L)	8.22	6.44	46
	DO (mg/L)	7.51	1.32	54
TCEQ-13563	TP (mg/L)	0.13	0.06	50
	NO_x (mg/L)	0.09	0.13	53
	TKN (mg/L)	0.94	0.37	49
	Chlorophyll-*a* (µg/L)	9.67	5.33	49
	DO (mg/L)	7.91	1.34	56

Watershed Nutrient Loads

Estimates of NO_3 and TP loads were developed using site and nutrient specific Generalized Additive Models (GAMs) relating nutrient concentration to river discharge, season, and time. Separate models were fit at each station for each parameter and used to predict nutrient concentrations for each day in the study period. GAMs can be specified in a functionally similar manner to the commonly used LOADEST (Cohn et al. 1992) or WRTDS (Hirsch et al. 2010) regression models and have been shown to produce reliable estimates of nutrient and sediment loadings (Wang et al. 2011; Kroon et al. 2012; Kuhnert et al. 2012; Robson and Dourdet 2015; Hagemann et al. 2016; McDowell et al. 2021; Biagi et al. 2022). GAMs are a semiparametric extension of generalized linear models where the linear predictor is represented as the sum of multiple unknown smooth functions and parametric linear predictors (Wood 2008). Although the underlying parameter

estimation procedure of GAMs is substantially different than WRTDS, both the functional form and results have been demonstrated to be similar (Beck and Murphy 2017). GAMs were chosen over other regression-based approached for use in this study due to; (1) the ability to easily explore and incorporate different model terms; (2) the incorporation of non-linear smooth functions that do not require explicit a priori knowledge of the expected shape; and (3) inclusion of a link function that related the expected value of the response to linear predictors thus avoiding unneeded data transformations and bias corrections.

GAMs were fit using the *mgcv* package in R which makes available multiple types of smooth functions with automatic smoothness selection (Wood 2008). The general form of the model related NO_3 or TP concentration to a long term tend, season, streamflow, and two different antecedent discharge terms:

$$g(\mu) = \alpha + f_1(\text{ddate}) + f_2(\text{yday}) + f_3\big(log1p(\text{Q})\big) + f_4(\text{ma}) + f_5(\text{fa})$$

$$y \sim \mathcal{N}(\mu, \sigma^2) \quad (1)$$

where μ is the conditional expected NO_3 or TP concentration, *g()* is the log-link, α is the intercept, $f_n()$ are smoothing functions. *y* is the response variable (NO_3 or TP concentration) modeled as normally distributed with mean μ and standard deviation σ. *ddate* is the date converted to decimal notation, *yday* is numeric day of year (1-366), and *log1p(Q)* is the natural log of mean daily streamflow plus 1.

Moving average (*ma*) is an exponentially smoothed moving average that attempts to incorporate the influence of prior streamflow events on concentration at the current time period [25,27,34]:

$$\text{ma}(\delta) = d\kappa_{i-1} + (1-\delta)\hat{q}_{i-1}, \kappa_i = \sum_{m=1}^{i} \hat{Q}_m \quad (2)$$

where δ is the discount factor (here, set equal to 0.95), κ_i is the cumulative flow (*Q*) up to the i^{th} day.

Flow anomaly (*fa*) is a unitless term that represents how wet or dry the current time period is from a previous time period (Vecchia et al. 2009; Zhang and Ball 2017). Long-term flow anomaly (*ltfa*) is the streamflow over the previous year relative to the entire period and calculated as described as (Zhang and Ball 2017):

$$\mathrm{ltfa}(t) = \bar{x}_{1\ \mathrm{year}}(t) - \bar{x}_{\mathrm{entire\ period}} \tag{3}$$

and the short-term flow anomaly (*stfa*) calculated as the current day flow compared to the preceding 1-month streamflow:

$$\mathrm{stfa}(t) = x_{\mathrm{current\ day}}(t) - \bar{x}_{1\ \mathrm{month}}(t) \tag{4}$$

where *x* are the averages of log-transformed streamflow over the antecedent period (1-year, 1-month, etc.) for time *t*. We used *ltfa* in NO_3 models and *stfa* in TP models based on previous work demonstrating major improvements in NO_x regression models that incorporated *ltfa* and moderate improvements in TP regression models that incorporated *stfa* (Zhang and Ball 2017).

The calculation of model terms for the Lake Texana site were slightly modified because daily loads are not a function of natural stream flow processes alone, but of dam releases and nutrient concentrations at the discharge point of the lake. *Q*, *ma*, and *fa* terms were calculated based on total gaged inflow from the four major tributaries to the lake. Thin-plate regression splines were used for *ddate*, *log1p(Q)*, *fa*, and *ma*. A cyclic cubic regression spline was used for *yday* to ensure the ends of the spline match (day 1 and day 366 are expected to match). First order penalties were applied to the smooths of flow-based variables which penalize departures from a flat function to help constrain extrapolations for high flow measurements.

Left-censored data were not uncommon in this dataset. Several methods are available to account for censored data, but for this study left-censored nutrient concentrations were transformed to one-half the detection limit. Although this simple approach can introduce bias (Hornung and Reed 1990), we considered it acceptable because high concentrations and loadings are associated with high-flow events and low-flow/low-concentration events will account for a small proportion of total loadings (McDowell et al. 2021).

Daily loads were estimated as the predicted concentration multiplied by the daily streamflow. For the Navidad River (USGS-08164525) site, daily loads at the dam were calculated from the discrete daily concentration at the discharge point of the lake and corresponding reported daily discharge from the dam. Flow-normalized loads were estimated similar to the WRTDS approach by setting flow-based covariates on each day of the year equal to each of the historical values for that day of the year over the study period [24]. The flow-normalized estimate was calculated as the mean of all the predictions for each day considering all possible flow values. Standard deviations and credible intervals were obtained by drawing samples from the multivariate normal posterior distribution of the fitted GAM (Wood 2006; Marra and Wood 2012; McDowell et al. 2021). Uncertainty in loads were calculated as 90% credible intervals estimated by drawing 1000 realizations of parameter estimates from the multivariate normal posterior distribution of the model parameters. GAM performance was evaluated using repeated 5-fold cross validation (Burman 1989) and average Nash-Sutcliffe Efficiency (NSE), r^2 and percent bias (PBIAS) metrics across folds were calculated for each model.

Linking Estuary Water Quality to Hydrology and Nutrient Loads

To test if changes in freshwater inflow and nutrient loading had explanatory effect on changes in estuary water quality a series of GAM models were fit at each site relating parameter concentration to temporal trends, inflow, and nutrient loads [40]:

$$g(\mu) = \alpha + f_1(\text{ddate}) + f_2(\text{yday})$$

$$y \sim \Gamma(\mu, \lambda) \quad (5)$$

$$g(\mu) = \alpha + f_1(\text{ddate}) + f_2(\text{yday}) + f_3(\text{Q})$$

$$y \sim \Gamma(\mu, \lambda) \quad (6)$$

$$g(\mu) = \alpha + f_1(\text{ddate}) + f_2(\text{yday}) + f_3(\text{Q}) + f_4(\text{Load})$$

$$y \sim \Gamma(\mu, \lambda) \quad (7)$$

where μ is the conditional expected response (nutrient concentration), *g()* is the log link, and response variable was modeled as Gamma distributed with mean μ and scale λ. f_1*(ddate)* is decimal date smoothed with a thin-plate regression spline, f_2*(yday)* is the numeric day of year smoothed with a cyclic cubic regression spline, f_3*(Q)* is mean daily inflow (the combined measurements from Lavaca River and Navidad River) and f_4*(Load)* is the total NO_3 or TP watershed load. The set of models specified for each water quality response are in Table 3.

Because streamflow and nutrient loads are tightly correlated, freshwater inflow can mask signals from nutrient loads alone. Prior work in the Chesapeake Bay accounted for this by preprocessing streamflow and load variables to account for season and flow (Murphy et al. 2022). In this study, freshwater inflow and nutrient loads were replaced by seasonally adjusted inflow and flow-adjusted nutrient loads obtained by fitting a GAM relating season (day of year) to log transformed daily freshwater inflow values:

$$g(\mu) = \alpha + f_1(\text{yday}) \quad (8)$$

and a GAM relating log transformed NO_3 or TP loads to log transformed daily inflow:

$$g(\mu) = \alpha + f_2\big(log(Q)\big) \quad (9)$$

where the response variables were modeled as normally distributed with an identity link function. Response residuals from the respective GAM models were used as *Q* and *Load* in Equation 6 and Equation 7.

An information theoretic approach was applied to evaluate if nutrient loads and/or freshwater inflows provided evidence of effects on water quality concentrations in Lavaca Bay. Model probabilities were calculated and compared using the AIC_c scores between each group of temporal, flow, and flow+load models (Burnham et al. 2011). Improvements in model probabilities provide evidence that the terms explain additional variation in the response variable. If model probabilities were tied, there wasn't evidence the more complicated model explains additional variation in water quality.

Results

Watershed Nutrient Loads

Individual models were generated for each site and parameter combination. Nutrient concentration model summaries (model coefficients and model metrics,) for each of those models are provided as tables in Appendix A. GAM models generally exhibited strong explanatory ability for NO_3 concentrations with adjusted r^2 values ranging from 0.717 to 0.965 and deviance explained values ranging from 0.767 to 0.977 (Figure 3). GAMs performed less well for explaining TP concentration with adjusted r^2 values ranging from 0.260 to 0.757 and deviance explained values between 0.323 and 0.824.

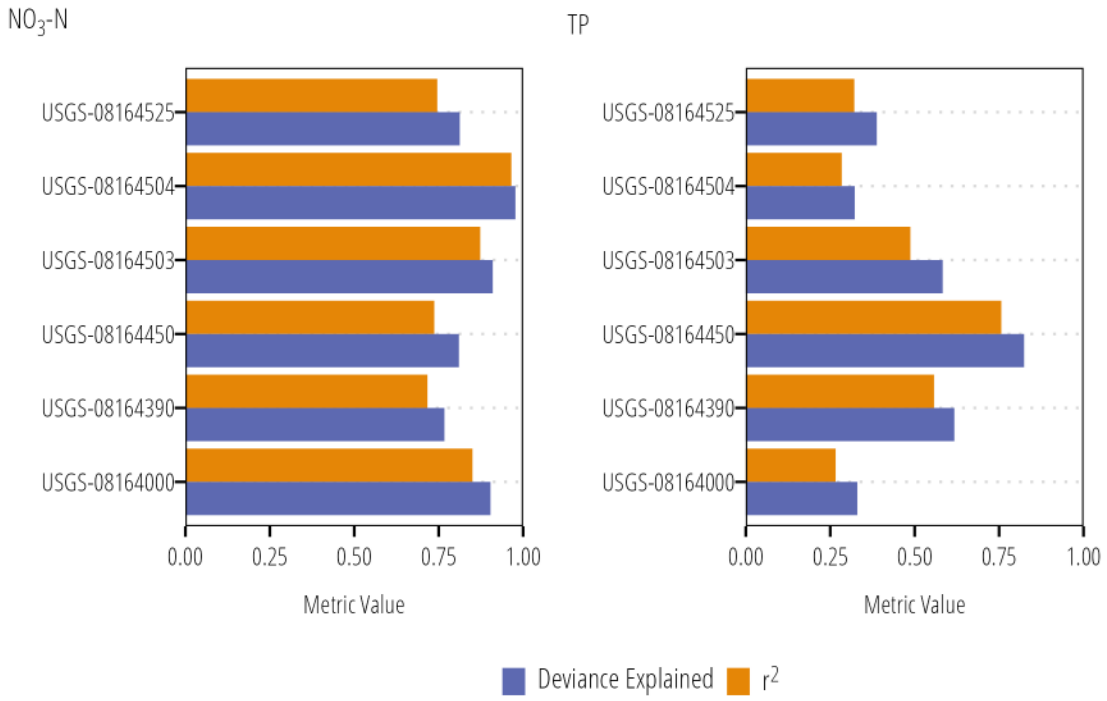

Figure 3. GAM model metrics for nutrient concentrations (r^2 and deviance explained) across each site and parameter.

Using evaluation criteria recommended by Moriasi et al. (2015), predictive performance of nutrient loading GAMs ranged from "satisfactory" to "very good" based on median NSE, r^2, and PBIAS metrics calculated using 5-fold cross validation. Median goodness-of-fit metrics for NO_3 models in the Lavaca River were 0.34 NSE, 0.70 r^2, and 2.00 PBIAS. NO_3 Navidad River appeared to perform slightly better with 0.48 NSE and 0.87 r^2 but with higher bias at 10.90 PBIAS. Generally, TP models performed better than the NO_3 models. Median goodness-of-fit metrics for TP models in the Lavaca River were 0.81 NSE, 0.93 r^2, and -7.20 PBIAS. TP models in the Navidad River had similar performance with 0.91 NSE, 0.99 r^2, and -3.30 PBIAS. Density plots of metrics show similar distribution of values between sites for the same parameter, with the exception r^2 values for NO_3 loads where Lavaca River had a much larger variance in values compared to the Navidad River (Figure

4). TP GAMS had higher average NSE and r^2 values and lower variance in metric values compared to NO_3.

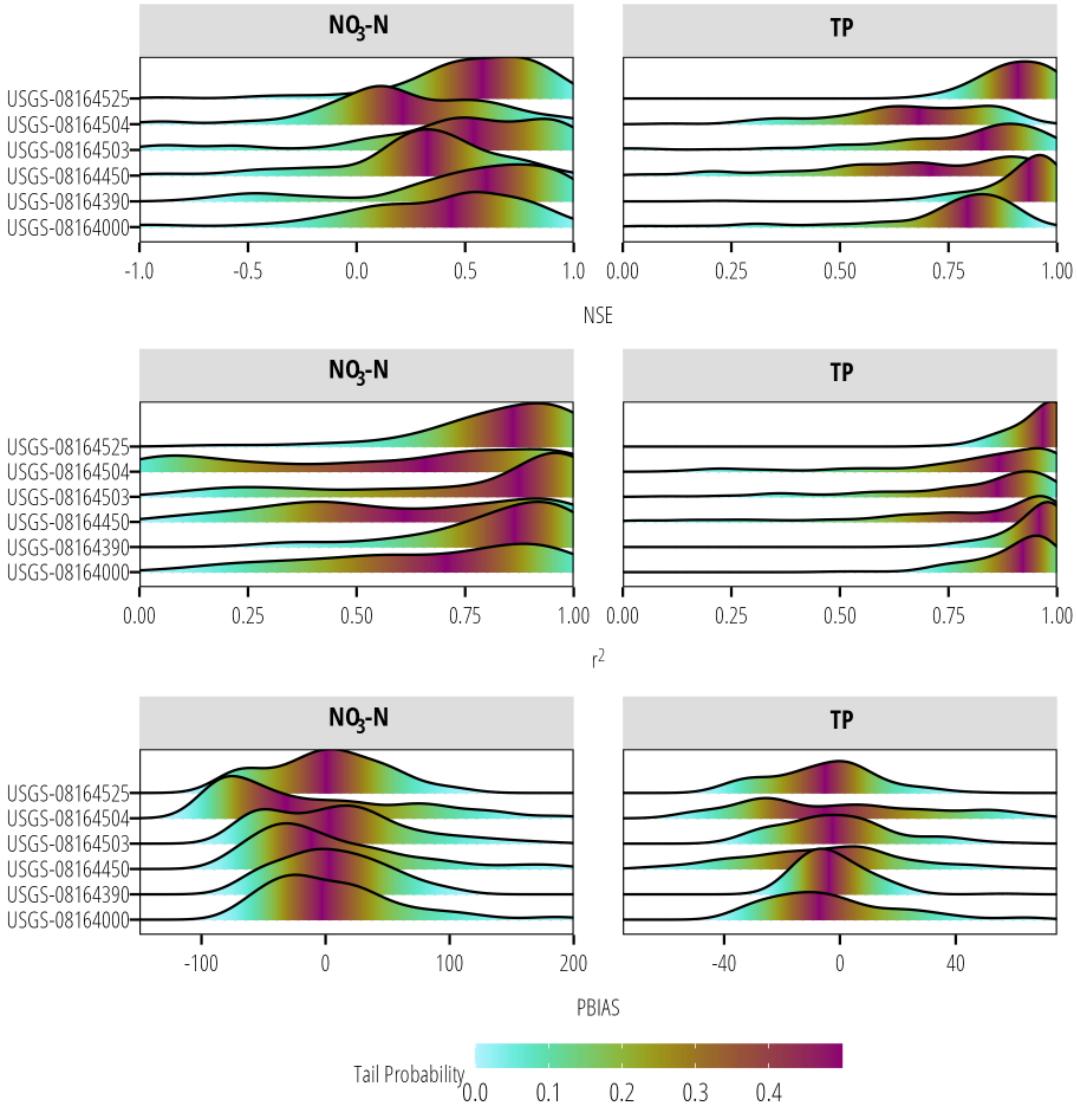

Figure 4. Density plots of goodness-of-fit metrics (NSE, r^2, and PBIAS) calculated from repeated 5-fold cross-validation between nutrient loads from GAM models and measured nutrient loads. Color indicates the tail probability calculated from the empirical cumulative distribution of the goodness-of-fit metrics.

Appendix B includes plots of predicted and flow-normalized loads for each site. Since the loads from the Lavaca River at USGS-08164000 and the Navidad River at USGS-08164525

serve as the inputs to Lavaca Bay, the remainder of the results section focuses on these two sites. Predicted annual NO_3 and TP loads show considerable variation, generally following patterns in discharge (Figure 5; Figure 6). Flow-normalized TP loads at both sites and the flow-normalized NO_3 loads in the Lavaca River indicated watershed-based loads did not change much over time when accounting for variation driven by streamflow (Figure 5). Flow-normalized loads in the Lavaca River showed small variation over time with some decreases in NO_3 loads since 2013.

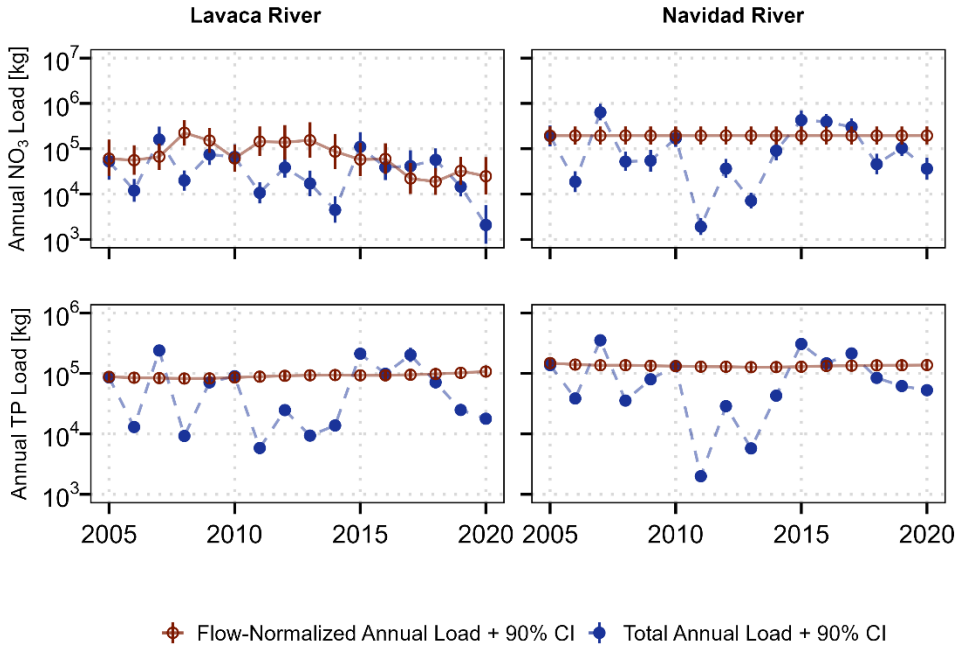

Figure 5. Aggregated annual and flow-normalized annual NO_3 and TP loads for the Lavaca River (USGS-08164000) and Navidad River (USGS-08164525).

Aggregated across both sites, the mean annual NO_3 load 2005 through 2020 was 205,405 kg (126,867 kg - 341,569 kg, 90% CI). Annual NO_3 loads ranged from 12,574 kg in 2011 to 794,510 kg in 2007. Total annual TP loads ranged from 7,839 kg in 2011 to 595,075 kg in 2007. Mean annual TP loading from 2005 through 2020 was 182,673 kg (152,227 kg - 219,310 kg, 90% CI). On average, the Navidad River accounted for 68% of NO_3 loads and

59% of TP loads from 2005 through 2020. However, during periods of extreme drought the Lavaca River became the primary source of nutrient loading in the watershed with the Navidad River only accounting for 15% and 25% of NO_3 and TP loads in 2011 (Figure 6).

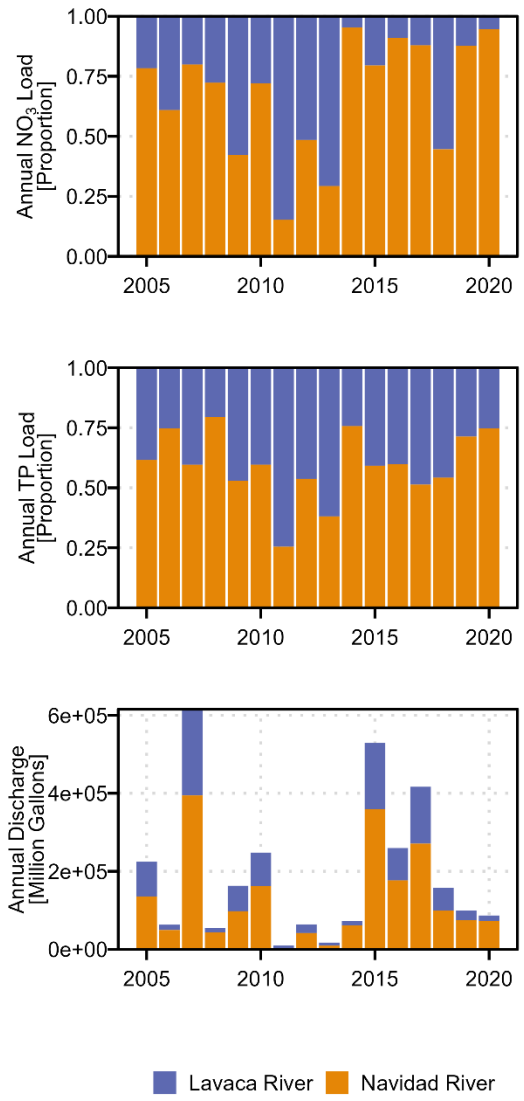

Figure 6. Comparisons of annual loads and annual discharge at the Lavaca River (USGS-08164000) and Navidad River (USGS-08164525).

Linkages Between Water Quality and Watershed Flows and Loads

GAMs did not identify significant changes in TP or DO concentrations at any of the Lavaca Bay sites from 2005 through 2020 (Figure 7). The upper-bay site, TCEQ-13563, had a linear increase in NO_x concentration and decrease in chlorophyll-*a* from 2005 through 2014. The mid-bay site, TCEQ-13383, showed a periodic pattern in NO_x concentration that appeared similar to precipitation/inflow patterns, as well as a post 2011 increase in TKN concentrations. No significant long-term trends in concentrations were identified by GAMs for the lower-bay TCEQ-13384 site.

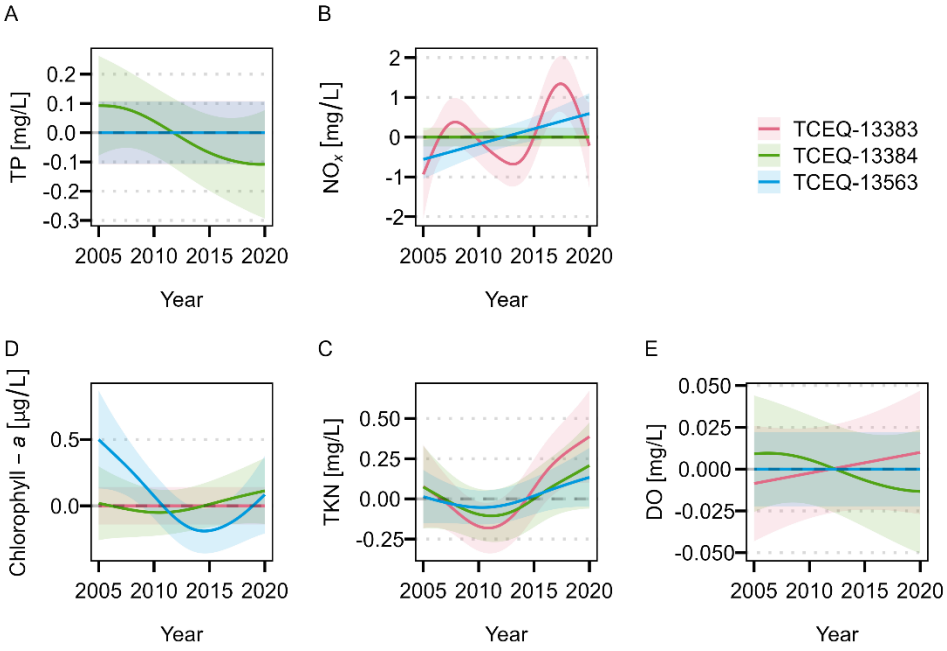

Figure 7. Effect of temporal predictor on estuary water quality concentration.

Freshwater inflow provided additional explanation for changes in TP and NO_x concentration at all of the Lavaca Bay sites according to AIC_c and model probability values (Table 3). TCEQ-13563, the site closest to the river outlet, was the only site that had improvements in the explanations of DO and TKN concentration with the inclusion of inflow. Both TCEQ-13563 and TCEQ-13383, the mid-bay site, saw improvements in

explanations for variations in chlorophyll-*a* with the inclusion of freshwater inflow. The addition of nutrient loads (both TP and NO_3) terms did not provide additional explanation for changes in chlorophyll-*a* or DO concentrations. Inclusion of TP loads provided additional explanation of TP concentrations at the upper- and mid-bay sites, TCEQ-13563 and TCEQ-13383. Inclusion of NO_3 loads only provided marginal improvements in the explanation of NO_x concentration at the lower-bay TCEQ-13384 site. Complete summaries of the estuary GAM models are included in Appendix C.

Table 3. Estuary GAM AIC_c values and associated model probabilities. Models with the highest probability for each site and water quality parameter combination are bolded and italicized for emphasis.

Parameter	Site	Temporal	Flow	Flow + Load
TP	TCEQ-13383	-152.1 (0.03)	-156.1 (0.24)	***-158.2 (0.72)***
	TCEQ-13384	-194.4 (0.03)	***-200.2 (0.49***)	-200.2 (0.49)
	TCEQ-13563	-145.3 (0)	-156.6 (0.41)	***-157.3 (0.59)***
NO_x	TCEQ-13383	-218.9 (0)	***-244.8 (0.5)***	-244.8 (0.5)
	TCEQ-13384	-263.4 (0)	-311.7 (0.48)	***-311.9 (0.52)***
	TCEQ-13563	-175.1 (0)	***-190.2 (0.5)***	-190.2 (0.5)
Chlorophyll-*a*	TCEQ-13383	279.7 (0.18)	***278.1 (0.41)***	278.1 (0.41)
	TCEQ-13384	***268.2 (0.33)***	268.2 (0.33)	268.2 (0.33)
	TCEQ-13563	289.5 (0.08)	***286.1 (0.46)***	286.1 (0.46)
TKN	TCEQ-13383	***42.2 (0.66)***	43.5 (0.34)	-
	TCEQ-13384	***34.3 (0.57)***	34.8 (0.43)	-
	TCEQ-13563	31.1 (0.22)	***28.7 (0.78)***	-
DO	TCEQ-13383	***146.4 (0.34)***	146.4 (0.34)	146.5 (0.32)
	TCEQ-13384	***135.9 (0.47)***	137 (0.27)	137 (0.27)
	TCEQ-13563	138.3 (0.25)	***137.2 (0.43)***	137.8 (0.32)

GAMs showed increases in freshwater inflow resulted in nearly linear increases in TP and NO_x concentration at all three sites (Figure 8). At the upper-bay TCEQ-13563 site, GAMs showed increases in freshwater inflow initially increased chlorophyll-*a* and DO concentration, but concentrations leveled and potentially decreased at higher flows. The mid-bay TCEQ-13383 site showed a nearly linear increased in chlorophyll-*a*

concentration in response to increases freshwater inflow. Freshwater flow did not have significant effects on chlorophyll-*a*, TKN, or DO at the lower-bay TCEQ-13384 site.

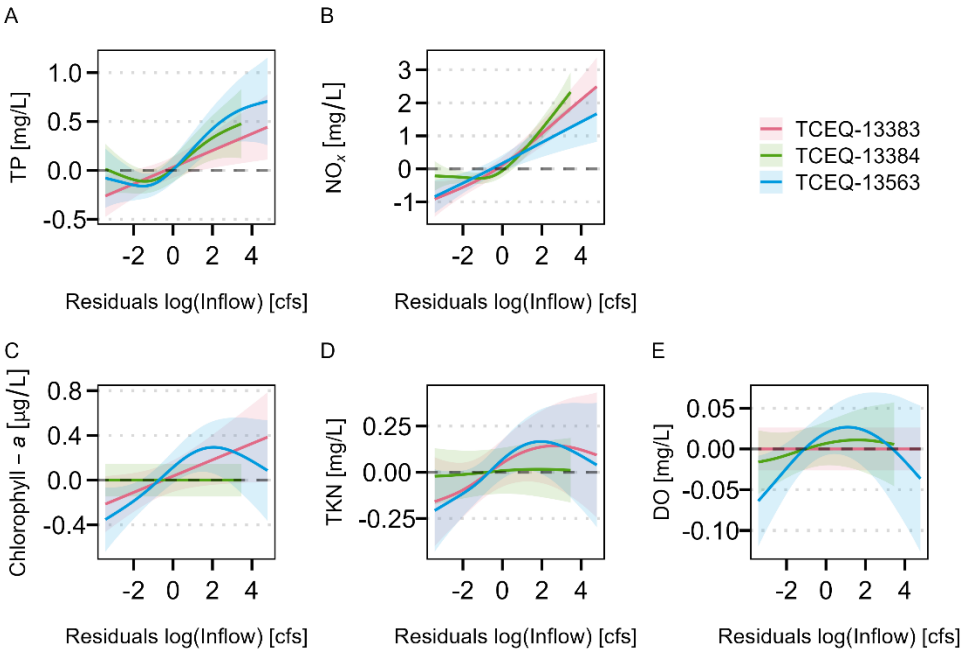

Figure 8. Effects of adjusted daily inflow on TP, NO_x, chlorophyll-*a*, TKN and DO in Lavaca Bay.

Increased TP loads resulted in nearly linear increases of TP concentration at the upper- and mid-bay sites, TCEQ-13563 and TCEQ-13383 respectively (Figure 9). The relative effect size appeared to be much smaller than the effect of freshwater inflow alone. Increased NO_3 loads only showed an effect at the lower-bay TCEQ-13384 site. The effect was quite small compared to streamflow and provided only small improvements to the model (Table 3). As noted above, nutrient loadings did not provide any explanation in changes in the remaining assessed water quality parameters.

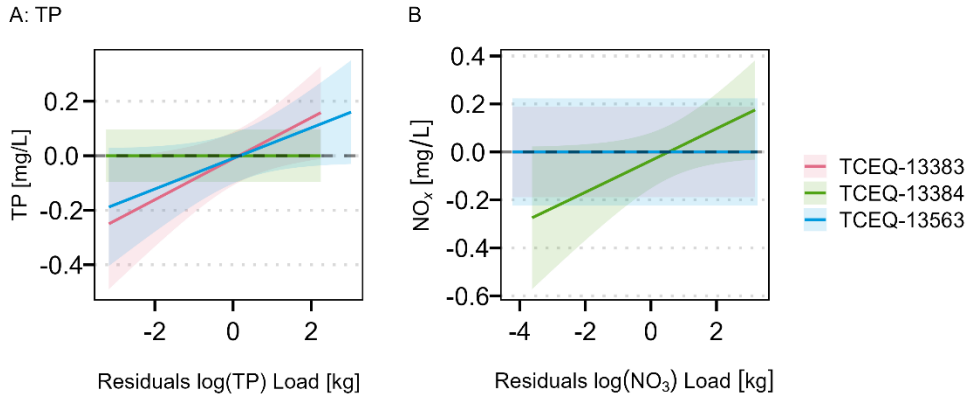

Figure 9. Effects of flow-adjusted nutrient loads on TP and NO_x in Lavaca Bay.

Discussion

This study faced two primary challenges for developing reliable estimates of nutrient loads; (1) relatively sparse nutrient concentration data collected approximately quarterly, and (2) application of statistical modelling approaches at a dam discharge site. Cross validation indicated GAMs performed well for predicting observed data at the mainstem Lavaca River and Lake Texana site. The variance in scores was very high indicating subsets of values were problematic at characterizing functional relationships between nutrients and predictors. Lower model performance at sites above Lake Texana suggests that higher resolution nutrient concentration data is needed to develop reliable estimates of nutrient loads. Under some conditions the log-linear relationship between streamflow and nutrient load, that is the underlying basis of the applied statistical approach, fail in these watersheds (East Mustang Creek and Sandy Creek in particular). East Mustang Creek has two upstream wastewater discharges (although no available daily nutrient discharge data) that might elevate instream nutrient concentrations under lower flow conditions, although not obvious relationships were discovered between quarterly reported discharges and measured instream concentration data. Compared to the Lavaca and Navidad Rivers, both East Mustang Creek and Sandy Creek watersheds are

dominated by cropped agricultural fields with little riparian buffer. Timing of fertilizer applications and precipitation may also have an unaccounted influence on instream nutrient concentrations. Finally, in these smaller streams, groundwater influence at low streamflows may have another unaccounted contribution to nutrient concentrations.

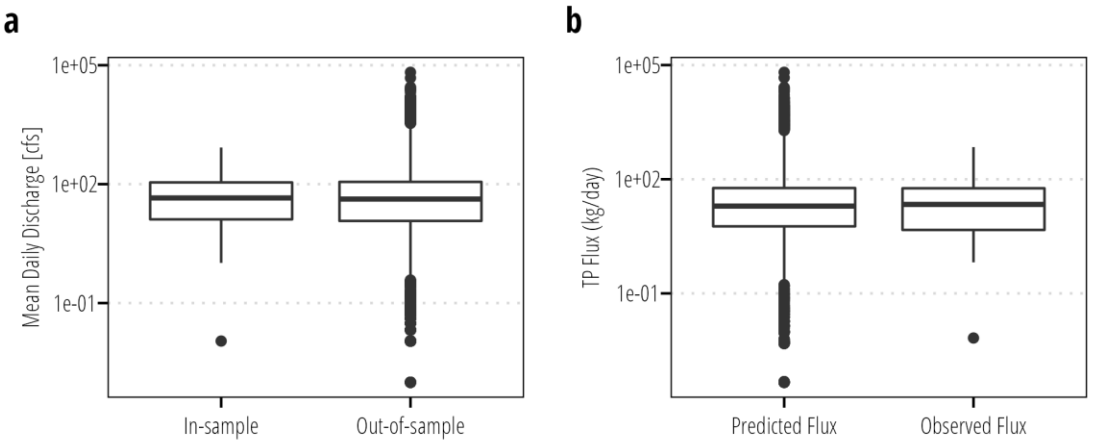

Figure 10. Comparisons of (a) in-sample and out-of-sample mean daily discharge and (b) predicted daily TP flux (load) and measured daily TP fluxes at Lavaca River (USGS-08164000).

Because all the water quality data for these two locations in the TCEQ databases were ambient water quality data, collected to be representative of typical flow conditions, there were few data at the highest portions of the flow-duration curve. It was beyond the scope of the current study to evaluate the subsets of cross-validation data and scores. However, the cross-validation procedure is indicative that more robust sampling would be beneficial for reducing prediction variance. Supplementary flow-biased monitoring targeting storm- or high-flow conditions is recommended here to improve the precision of GAM predictions (Horowitz 2003; Snelder et al. 2017). Figure 10a shows the distribution of streamflow represented by TP samples collected under the routine monitoring program at Lavaca River (USGS-08164000). The collected data is well representative of the median and 25th - 75th interquartile range of mean daily streamflow values at this site. High flow conditions are responsible for most of total nutrient loadings

in watersheds. In order to develop accurate estimates of high flow loadings using regression-based approaches, supplemental flow-biased nutrient concentration data should be collected to supplement existing data. Figure 10b shows the distribution of predicted daily TP flux and observed flux at Lavaca River (USGS-08164000). The distribution of observed daily fluxes shows that there are no measured observations of extreme nutrient loading events (greater than 1.5 times the 75 percentile). This makes it impossible to confirm the accuracy of important high load events. The importance of including flow-biased or storm sampling in regression-based load estimates has been confirmed by Vieux and Moreda (2003), Snelder (2017), and Zhang and Ball (2017).

Converted to average annual yield, the estimate of annual TP loads for the Lavaca River are within the ranges in previous published studies (Table 4) (Dunn 1996; Rebich et al. 2011; Omani et al. 2014; Wise et al. 2019). It isn't obvious why the TP estimate by Dunn (1996) is notably lower. Given that none of the studies identify substantially sized trends in TP, it is possible that the period used in Dunn (1996) was drier on average than the other studies. The SPARROW models used in by Rebich et al. (2011) and Wise et al. (2019) utilize a version of LOADEST in the underlying load estimation procedure, so a difference due to methodology alone is unlikely.

Table 4. Comparisons of previously published estimates of mean annal TP yield at the Lavaca River site.

Reported Yield (kg · km^{-2} · year^{-1})	Approach	Time Period	Reference
35.2 (28.8, 43.3)[a]	GAM	2005-2020	This work
45.2	SPARROW	2000-2014	(Wise et al. 2019)
42	SWAT	1977-2005	(Omani et al. 2014)
20.81-91.58[b]	SPARROW	1980-2002	(Rebich et al. 2011)
28.9	LOADEST	1972-1993	(Dunn 1996)

[a]Values represent the mean of annual point estimates, lower and upper 95% credible intervals.
[b]A single point estimate was not reported, these values represent the range depicted on the choropleth map provided in the report.

The flexibility of the GAM approach allowed us to easily incorporate inflow-based covariates at the Lake Texana site and antecedent discharge conditions at all sites. Model

summaries (Appendix A) indicate many of these covariates provide explanatory information. Another advantage of the GAM approach is the ability to use different exponential families for the conditional response. We used the Gaussian distribution with a log link in this study based on exploratory work that found that Tobit I and censored Gamma families did not perform as well. However, due to the prevalence of left-censored data, future work should investigate the use of families that accommodate censored responses. This might improve predictive ability and better align with best practices for utilizing censored data (Helsel 2006).

Both NO_3 and TP loadings show high annual, monthly, and daily variability driven by the amount of freshwater discharge in the system. Discharge as measured at the Lavaca River USGS gauge is largely unmodified and representative a fairly natural system with minimal withdrawals, wastewater contributions, or dams. Conversely, the Palmetto Bend Dam forming Lake Texana on the Navidad River is representative of a highly regulated system. From 2005 through 2020 the Navidad River/Lake Texana system contributed 68% of NO_3 and 59% of TP loadings to Lavaca Bay from the Lavaca River/Navidad river system. The Lavaca and Navidad watersheds account for approximately 73% of the Lavaca Bay watershed land area. Additional nutrient contributions to Lavaca Bay from the Garcitas Creek, Placedo Creek, and Cox Bay watersheds are not accounted for due to lack of measured nutrient concentration data in those watersheds.

There is little evidence for changes in flow-normalized TP loads in either river. There is some evidence of recent decreases in flow-normalized NO_3 loads in the Lavaca River. Although there is no work directly correlating water quality planning and implementation efforts in the watershed to water quality outcomes, efforts to increase agricultural producer participation in the watershed have been ongoing since 2016 (Schramm et al. 2018; Berthold et al. 2021). The decrease in flow-normalized NO_3 loads

could be a reflection of those collective efforts but further data collection and research is required to support that statement.

The non-linear temporal water quality trends identified using GAMs differed slightly from previously identified trends (Bugica et al. 2020). This is not unexpected due to the different time periods, different methodology, and generally small slopes previously identified for most of the significant water quality parameters. The trend in DO and chlorophyll-*a* concentrations are stable in comparison to other Texas estuaries that are facing larger demands for freshwater diversions, higher population growth, and more intense agricultural production (Wetz et al. 2016; Bugica et al. 2020). The trend of increasing NO_x concentration at the upper-bay TCEQ-13563 site and recent increases in TKN concentration at the mid-bay TCEQ-13383 site are concerning due to the nitrogen limitation identified in many Texas estuaries (Hou et al. 2012; Dorado et al. 2015; Wetz et al. 2017; Paudel et al. 2019) and the relatively low ambient concentrations observed in Lavaca Bay.

The strong positive effect of freshwater inflow on NO_x, TKN, and TP are suggestive of nonpoint watershed sources, consistent with watershed uses and with other studies relating freshwater inflow with nutrient concentrations in Lavaca Bay and other estuaries (Russell et al. 2006; Caffrey et al. 2007; Peierls et al. 2012; Palmer and Montagna 2015; Cira et al. 2021). Inflow had a non-linear relationship with TKN at the two upstream sites, with TKN increasing as freshwater inflow transitioned from low to moderate levels. At higher freshwater inflows, the effect was attenuated, possibly indicating a flushing effect at higher freshwater inflow. No relationship between TKN and freshwater inflow were observed at TCEQ-13384 located in the lower reach of Lavaca Bay. Tidal flushing from Matagorda Bay could be responsible for diluting TKN and acting as a control on the effects of freshwater inflow in lower reaches of Lavaca Bay. Previous work suggests the

processing of organic loads in the upper portions of Lavaca Bay might reduce the transport of nutrients into the lower reaches of the Bay (Russell et al. 2006).

Freshwater inflow had a strong positive effect on chlorophyll-*a* at the upper- and mid-bay sites. The upper-bay site, TCEQ-13563, showed decreases in chlorophyll-*a* at the highest freshwater inflow volumes. Freshwater flushing or increases in turbidity are associated with decreases in chlorophyll-*a* in other estuaries (Peierls et al. 2012; Cloern et al. 2014). No relationships between inorganic nitrogen or TP loadings with chlorophyll-*a* were observed. Due to the lack of TKN loading information, no assessment between organic nitrogen loads and chlorophyll-*a* were possible.

Although other studies have identified complex relationships between estuary nutrient concentrations, nutrient loading and chlorophyll-*a* concentrations in Texas estuaries (Örnólfsdóttir et al. 2004; Dorado et al. 2015; Cira et al. 2021; Tominack and Wetz 2022 Nov 14), this study specifically used flow-adjusted freshwater derived nutrient loads to parse out contributions from changes in nutrient loadings while accounting for variations in load due to flow. Nutrient loading GAMs indicated no evidence of changes in flow-normalized TP loads in either river and no changes in flow-normalized NO_3 loads in the Navidad River. The small changes in flow-normalized NO_3 loads in the Lavaca River are probably masked under most conditions by discharge from the Navidad River. Given the relatively small variation in flow-normalized loads, it can be expected that they would contribute little to the variance in downstream water quality.

GAMs did not identify responses in DO concentration to inflows or nutrient loads. The seasonality term in the temporal GAM models explained a substantial amount of DO variation at all of the sites. Responses of estuary metabolic processes and resulting DO concentrations can be quite complicated and often locally specific (Caffrey 2004). While the lack of total nitrogen or TKN loading data hinders interpretation, the large seasonal effect on DO suggests physical factors play an important role and should be included in

future models. Prior work suggests that Lavaca Bay may not be limited by nutrients alone, with high turbidity or nutrient processing in upper portions of the Bay or intertidal river limiting production (Russell et al. 2006). Finally, it is reasonable to assume that fluctuations in DO may not occur immediately in response to nutrient pulses or freshwater inflow. Work has shown that various water quality parameters may have lagged effects lasting days or even months following storms and large discharge events (Mooney and McClelland 2012; Wetz and Yoskowitz 2013; Bukaveckas et al. 2020; Walker et al. 2021). However, our work only evaluates responses to loading and inflows occurring the day of water quality observations.

Conclusion

The study approach appears to provide reliable estimates of nutrient loads in the Lavaca Bay watershed despite data shortcomings. Presumably this approach will be suited to other coastal estuaries with limited data although additional flow-biased data collection should be pursued to better understand model performance under high flow conditions. Ongoing projects are filling other data gaps regarding total nitrogen and TKN loadings.

This study, consistent with others along the Texas coast, found strong effects of freshwater flow on nutrient and chlorophyll-*a* concentrations. DO concentrations, dominated by seasonal effects, did not show strong direct responses to freshwater flow. Small variance in flow-adjusted nutrient loads indicates that (1) there have been limited changes in non-point sources of nutrients and (2) that there isn't strong evidence that those small changes have had effects on chlorophyll-*a* or dissolved oxygen in Lavaca Bay. Although the study did not identify strong responses to changes in nutrient loading, this does provide a baseline assessment for future water quality management activities in the watershed. The type of nutrient loading data generated by this project might be more

informative in watersheds where strong land use changes or increases in point source discharges have taken place.

Bibliography

Beck MW, Murphy RR. 2017. Numerical and qualitative contrasts of two statistical models for water quality change in tidal waters. JAWRA J Am Water Resour Assoc. 53(1):197–219. doi:10.1111/1752-1688.12489.

Berthold TA, Olsovsky T, Schramm MP. 2021. Direct mailing education campaign impacts on the adoption of grazing management practices. J Contemp Water Res Educ.(174):45–60. doi:10.1111/j.1936-704X.2021.3360.x.

Beseres Pollack J, Palmer T, Montagna P. 2011. Long-term trends in the response of benthic macrofauna to climate variability in the Lavaca-Colorado Estuary, Texas. Mar Ecol Prog Ser. 436:67–80. doi:10.3354/meps09267.

Biagi KM, Ross CA, Oswald CJ, Sorichetti RJ, Thomas JL, Wellen CC. 2022. Novel predictors related to hysteresis and baseflow improve predictions of watershed nutrient loads: An example from Ontario's lower Great Lakes basin. Sci Total Environ. 826:154023. doi:10.1016/j.scitotenv.2022.154023.

Bricker SB, Longstaff B, Dennison W, Jones A, Boicourt K, Wicks C, Woerner J. 2008. Effects of nutrient enrichment in the nation's estuaries: A decade of change. Harmful Algae. 8(1):21–32. doi:10.1016/j.hal.2008.08.028.

Bugica K, Sterba-Boatwright B, Wetz MS. 2020. Water quality trends in Texas estuaries. Mar Pollut Bull. 152:110903. doi:10.1016/j.marpolbul.2020.110903.

Bukaveckas PA, Tassone S, Lee W, Franklin RB. 2020. The influence of storm events on metabolism and water quality of riverine and estuarine segments of the James, Mattaponi, and Pamunkey Rivers. Estuaries Coasts. 43(7):1585–1602. doi:10.1007/s12237-020-00819-9.

Burman P. 1989. A comparative study of ordinary cross-validation, v-fold cross-validation and the repeated learning-testing methods. Biometrika. 76(3):503–514. doi:10.1093/biomet/76.3.503.

Burnham KP, Anderson DR, Huyvaert KP. 2011. AIC model selection and multimodel inference in behavioral ecology: some background, observations, and comparisons. Behav Ecol Sociobiol. 65(1):23–35. doi:10.1007/s00265-010-1029-6.

Caffrey JM. 2004. Factors controlling net ecosystem metabolism in U.S. estuaries. Estuaries. 27(1):90–101. doi:10.1007/BF02803563.

Caffrey JM, Chapin TP, Jannasch HW, Haskins JC. 2007. High nutrient pulses, tidal mixing and biological response in a small California estuary: Variability in nutrient concentrations from decadal to hourly time scales. Estuar Coast Shelf Sci. 71(3–4):368–380. doi:10.1016/j.ecss.2006.08.015.

Chin T, Beecraft L, Wetz MS. 2022. Phytoplankton biomass and community composition in three Texas estuaries differing in freshwater inflow regime. Estuar Coast Shelf Sci. 277:108059. doi:10.1016/j.ecss.2022.108059.

Cira EK, Palmer TA, Wetz MS. 2021. Phytoplankton dynamics in a low-inflow estuary (Baffin Bay, TX) during drought and high-rainfall conditions associated with an El Niño event. Estuaries Coasts. 44(7):1752–1764. doi:10.1007/s12237-021-00904-7.

Cloern JE, Foster SQ, Kleckner AE. 2014. Phytoplankton primary production in the world's estuarine-coastal ecosystems. Biogeosciences. 11(9):2477–2501. doi:10.5194/bg-11-2477-2014.

Cohn TA, Caulder DL, Gilroy EJ, Zynjuk LD, Summers RM. 1992. The validity of a simple statistical model for estimating fluvial constituent loads: An empirical study involving nutrient loads entering Chesapeake Bay. Water Resour Res. 28(9):2353–2363. doi:10.1029/92WR01008.

De Cicco LA, Hirsch RM, Lorenz DL, Watkins WD, Johnson M. 2022. dataRetrieval: R packages for discovering and retrieving water data available from Federal hydrologic web services. https://code.usgs.gov/water/dataRetrieval.

Dorado S, Booe T, Steichen J, McInnes AS, Windham R, Shepard A, Lucchese AEB, Preischel H, Pinckney JL, Davis SE, et al. 2015. Towards an understanding of the interactions between freshwater inflows and phytoplankton communities in a subtropical estuary in the Gulf of Mexico. PLOS ONE. 10(7):e0130931. doi:10.1371/journal.pone.0130931.

Dunn D. 1996. Trends in Nutrient Inflows to the Gulf of Mexico from Streams Draining the Conterminous United States, 1972-93. Austin, Texas: USGS Report No.: 96–4113. http://pubs.er.usgs.gov/publication/wri964113.

Gardner WS, McCarthy MJ, An S, Sobolev D, Sell KS, Brock D. 2006. Nitrogen fixation and dissimilatory nitrate reduction to ammonium (DNRA) support nitrogen dynamics in Texas estuaries. Limnol Oceanogr. 51(1part2):558–568. doi:10.4319/lo.2006.51.1_part_2.0558.

Hagemann M, Kim D, Park MH. 2016. Estimating nutrient and organic carbon loads to water-supply reservoir using semiparametric models. J Environ Eng. 142(8):04016036. doi:10.1061/(ASCE)EE.1943-7870.0001077.

Helsel DR. 2006. Fabricating data: How substituting values for nondetects can ruin results, and what can be done about it. Chemosphere. 65(11):2434–2439. doi:10.1016/j.chemosphere.2006.04.051.

Hirsch RM, Moyer DL, Archfield SA. 2010. Weighted Regressions on Time, Discharge, and Season (WRTDS), with an application to Chesapeake Bay River inputs. JAWRA J Am Water Resour Assoc. 46(5):857–880. doi:10.1111/j.1752-1688.2010.00482.x.

Hornung RW, Reed LD. 1990. Estimation of average concentration in the presence of nondetectable values. Appl Occup Environ Hyg. 5(1):46–51. doi:10.1080/1047322X.1990.10389587.

Horowitz AJ. 2003. An evaluation of sediment rating curves for estimating suspended sediment concentrations for subsequent flux calculations. Hydrol Process. 17(17):3387–3409. doi:10.1002/hyp.1299.

Hou L, Liu M, Carini SA, Gardner WS. 2012. Transformation and fate of nitrate near the sediment–water interface of Copano Bay. Cont Shelf Res. 35:86–94. doi:10.1016/j.csr.2012.01.004.

Jain S, Schramm MP. 2021. Technical Support Document for One Total Maximum Daily Load for Indicator Bacteria in Lavaca River Above Tidal. Austin, Texas: Texas Commission on Environmental Quality Report No.: AS-221. https://www.tceq.texas.gov/downloads/water-quality/tmdl/lavaca-river-above-tidal-rocky-creek-recreational-108/108-lavaca-river-addendum-tsd-2021-october-as-221.pdf.

Kennicutt MC. 2017. Water Quality of the Gulf of Mexico. In: Ward CH, editor. Habitats and Biota of the Gulf of Mexico: Before the Deepwater Horizon Oil Spill. New York, NY: Springer New York. p. 55–164. http://link.springer.com/10.1007/978-1-4939-3447-8_2.

Kroon FJ, Kuhnert PM, Henderson BL, Wilkinson SN, Kinsey-Henderson A, Abbott B, Brodie JE, Turner RDR. 2012. River loads of suspended solids, nitrogen, phosphorus and herbicides delivered to the Great Barrier Reef lagoon. Mar Pollut Bull. 65(4–9):167–181. doi:10.1016/j.marpolbul.2011.10.018.

Kuhnert PM, Henderson BL, Lewis SE, Bainbridge ZT, Wilkinson SN, Brodie JE. 2012. Quantifying total suspended sediment export from the Burdekin River catchment using

the loads regression estimator tool. Water Resour Res. 48(4). doi:10.1029/2011WR011080.

Lloyd CEM, Freer JE, Collins AL, Johnes PJ, Jones JI. 2014. Methods for detecting change in hydrochemical time series in response to targeted pollutant mitigation in river catchments. J Hydrol. 514:297–312. doi:10.1016/j.jhydrol.2014.04.036.

Marra G, Wood SN. 2012. Coverage properties of confidence intervals for Generalized Additive Model components: Coverage properties of GAM intervals. Scand J Stat. 39(1):53–74. doi:10.1111/j.1467-9469.2011.00760.x.

McDowell RW, Simpson ZP, Ausseil AG, Etheridge Z, Law R. 2021. The implications of lag times between nitrate leaching losses and riverine loads for water quality policy. Sci Rep. 11(1):16450. doi:10.1038/s41598-021-95302-1.

Montagna PA, Cockett PM, Kurr EM, Trungale J. 2020. Assessment of the Relationship Between Freshwater Inflow and Biological Indicators in Lavaca Bay. Corpus Christi, Texas: Harte Research Institute, Texas A&M University-Corpus Christi Final Report to the Texas Water Development Board Report No.: Contract # 1800012268.

Mooney RF, McClelland JW. 2012. Watershed export events and ecosystem responses in the Mission–Aransas National Estuarine Research Reserve, South Texas. Estuaries Coasts. 35(6):1468–1485. doi:10.1007/s12237-012-9537-4.

Moriasi DN, Gitau MW, Pai N, Daggupati P. 2015. Hydrologic and Water Quality Models: Performance Measures and Evaluation Criteria. Trans ASABE. 58(6):1763–1785. doi:10.13031/trans.58.10715.

Murphy RR, Keisman J, Harcum J, Karrh RR, Lane M, Perry ES, Zhang Q. 2022. Nutrient improvements in Chesapeake Bay: Direct effect of load reductions and implications for coastal management. Environ Sci Technol. 56(1):260–270. doi:10.1021/acs.est.1c05388.

Omani N, Srinivasan R, Lee T. 2014. Estimation of sediment and nutrient loads to bays from gauged and ungauged watersheds. Appl Eng Agric.:869–887. doi:10.13031/aea.30.10162.

Örnólfsdóttir EB, Lumsden SE, Pinckney JL. 2004. Nutrient pulsing as a regulator of phytoplankton abundance and community composition in Galveston Bay, Texas. J Exp Mar Biol Ecol. 303(2):197–220. doi:10.1016/j.jembe.2003.11.016.

Palmer TA, Montagna PA. 2015. Impacts of droughts and low flows on estuarine water quality and benthic fauna. Hydrobiologia. 753(1):111–129. doi:10.1007/s10750-015-2200-x.

Paudel B, Montagna PA, Adams L. 2019. The relationship between suspended solids and nutrients with variable hydrologic flow regimes. Reg Stud Mar Sci. 29:100657. doi:10.1016/j.rsma.2019.100657.

Peierls BL, Hall NS, Paerl HW. 2012. Non-monotonic responses of phytoplankton biomass accumulation to hydrologic variability: A comparison of two coastal plain North Carolina estuaries. Estuaries Coasts. 35(6):1376–1392. doi:10.1007/s12237-012-9547-2.

Rebich RA, Houston NA, Mize SV, Pearson DK, Ging PB, Evan Hornig C. 2011. Sources and delivery of nutrients to the northwestern Gulf of Mexico from streams in the south-central United States. JAWRA J Am Water Resour Assoc. 47(5):1061–1086. doi:10.1111/j.1752-1688.2011.00583.x.

Robson BJ, Dourdet V. 2015. Prediction of sediment, particulate nutrient and dissolved nutrient concentrations in a dry tropical river to provide input to a mechanistic coastal water quality model. Environ Model Softw. 63:97–108. doi:10.1016/j.envsoft.2014.08.009.

Russell MJ, Montagna PA, Kalke RD. 2006. The effect of freshwater inflow on net ecosystem metabolism in Lavaca Bay, Texas. Estuar Coast Shelf Sci. 68(1–2):231–244. doi:10.1016/j.ecss.2006.02.005.

Schramm M, Berthold A, Entwistle C, Peddicord K. 2018. Lavaca River Watershed Protection Plan. College Station, Texas: Texas Water Resources Institute Report No.: TR-507. https://twri.tamu.edu/media/1456/tr-507.pdf.

Schramm MP, Gitter A, Gregory L. 2022. Total Maximum Daily Loads and *Escherichia coli* trends in Texas freshwater streams. J Contemp Water Res Educ.(176):36–49. doi:10.1111/j.1936-704X.2022.3374.x.

Snelder TH, McDowell RW, Fraser CE. 2017. Estimation of catchment nutrient loads in New Zealand using monthly water quality monitoring data. JAWRA J Am Water Resour Assoc. 53(1):158–178. doi:10.1111/1752-1688.12492.

Tominack SA, Wetz MS. 2022 Nov 14. Variability in phytoplankton biomass and community composition in Corpus Christi Bay, Texas. Estuaries Coasts. doi:10.1007/s12237-022-01137-y.

Vecchia AV, Gilliom RJ, Sullivan DJ, Lorenz DL, Martin JD. 2009. Trends in concentrations and use of agricultural herbicides for Corn Belt Rivers, 1996–2006. Environ Sci Technol. 43(24):9096–9102. doi:10.1021/es902122j.

Vieux BE, Moreda FG. 2003. Nutrient loading assessment in the Illinois River using a synthetic approach. J Am Water Resour Assoc. 39(4):757–769. doi:10.1111/j.1752-1688.2003.tb04403.x.

Walker LM, Montagna PA, Hu X, Wetz MS. 2021. Timescales and magnitude of water quality change in three Texas estuaries induced by passage of Hurricane Harvey. Estuaries Coasts. 44(4):960–971. doi:10.1007/s12237-020-00846-6.

Wang Y-G, Kuhnert P, Henderson B. 2011. Load estimation with uncertainties from opportunistic sampling data – A semiparametric approach. J Hydrol. 396(1–2):148–157. doi:10.1016/j.jhydrol.2010.11.003.

Wazniak CE, Hall MR, Carruthers TJB, Sturgis B, Dennison WC, Orth RJ. 2007. Linking water quality to living resources in a Mid-Atlantic lagoon system, USA. Ecol Appl. 17(sp5):S64–S78. doi:10.1890/05-1554.1.

Wetz MS, Cira EK, Sterba-Boatwright B, Montagna PA, Palmer TA, Hayes KC. 2017. Exceptionally high organic nitrogen concentrations in a semi-arid South Texas estuary susceptible to brown tide blooms. Estuar Coast Shelf Sci. 188:27–37. doi:10.1016/j.ecss.2017.02.001.

Wetz MS, Hayes KC, Fisher KVB, Price L, Sterba-Boatwright B. 2016. Water quality dynamics in an urbanizing subtropical estuary(Oso Bay, Texas). Mar Pollut Bull. 104(1–2):44–53. doi:10.1016/j.marpolbul.2016.02.013.

Wetz MS, Yoskowitz DW. 2013. An 'extreme' future for estuaries? Effects of extreme climatic events on estuarine water quality and ecology. Mar Pollut Bull. 69(1–2):7–18. doi:10.1016/j.marpolbul.2013.01.020.

Wise DR, Anning DW, Miller OW. 2019. Spatially referenced models of streamflow and nitrogen, phosphorus, and suspended-sediment transport in streams of the southwestern United States. Reston, Virginia: U.S. Geological Survey Scientific Investigations Report Report No.: 2019–5106. https://doi.org/10.3133/sir20195106.

Wood SN. 2006. On confidence intervals for generalized additive models based on penalized regression splines. Aust N Z J Stat. 48(4):445–464. doi:10.1111/j.1467-842X.2006.00450.x.

Wood SN. 2008. Fast stable direct fitting and smoothness selection for generalized additive models. J R Stat Soc Ser B Stat Methodol. 70(3):495–518. doi:10.1111/j.1467-9868.2007.00646.x.

Zhang Q, Ball WP. 2017. Improving riverine constituent concentration and flux estimation by accounting for antecedent discharge conditions. J Hydrol. 547:387–402. doi:10.1016/j.jhydrol.2016.12.052.

Appendix A: Freshwater Site Model Summaries

GAM model summaries report smoothness selection for model parameters, approximate p-values of smoothed parameters, deviance explained (the proportion of the null deviance explained by the model), and model adjusted r^2 (proportion of variance explained) of the final full fitted GAM model.

Table 5. Lavaca River (USGS-08164000) GAM summary for NO_3.

Component	Term	Estimate	Std Error	t-value	p-value	
A. parametric coefficients	(Intercept)	-2.346	0.152	-15.390	0.0000	***
Component	**Term**	**edf**	**Ref. df**	**F-value**	**p-value**	
B. smooth terms	s(ddate)	10.465	17.000	4.598	0.0000	***
	s(yday)	2.400	4.000	6.578	0.0000	***
	s(log1p_Flow)	5.968	9.000	4.521	0.0000	***
	s(ma)	0.003	9.000	0.000	0.3332	
	s(ltfa)	7.144	9.000	6.180	0.0000	***

Signif. codes: 0 <= '***' < 0.001 < '**' < 0.01 < '*' < 0.05

Adjusted R-squared: 0.850, Deviance explained 0.903

-REML : -28.133, Scale est: 0.00876, N: 74

Table 6. Lavaca River (USGS-08164000) GAM summary for TP.

Component	Term	Estimate	Std Error	t-value	p-value	
A. parametric coefficients	(Intercept)	-1.581	0.044	-35.749	0.0000	***
Component	**Term**	**edf**	**Ref. df**	**F-value**	**p-value**	
B. smooth terms	s(ddate)	3.140	17.000	0.346	0.0834	.
	s(yday)	0.845	8.000	0.173	0.1847	
	s(log1p_Flow)	0.000	4.000	0.000	0.4413	
	s(ma)	0.000	5.000	0.000	0.5359	
	s(stfa)	3.012	4.000	6.167	0.0000	***

Signif. codes: 0 <= '***' < 0.001 < '**' < 0.01 < '*' < 0.05

Adjusted R-squared: 0.266, Deviance explained 0.330

-REML : -80.284, Scale est: 0.00644, N: 80

Table 7. Lake Texana at Palmetto Bend Dam (USGS-08164525) GAM summary for NO_3.

Component	Term	Estimate	Std Error	t-value	p-value	
A. parametric coefficients	(Intercept)	-1.450	0.087	-16.634	0.0000	***
Component	**Term**	**edf**	**Ref. df**	**F-value**	**p-value**	
B. smooth terms	s(ddate)	0.000	9.000	0.000	0.7788	
	s(yday)	2.836	8.000	5.179	0.0000	***
	s(log1p_inflow)	0.000	4.000	0.000	0.4670	
	s(log1p_Flow)	6.058	9.000	2.712	0.0004	***
	s(ma)	2.665	5.000	2.101	0.0022	**
	s(ltfa)	4.781	9.000	3.193	0.0000	***

Signif. codes: 0 <= '***' < 0.001 < '**' < 0.01 < '*' < 0.05

Adjusted R-squared: 0.746, Deviance explained 0.812

-REML : -15.004, Scale est: 0.017, N: 62

Table 8. Lake Texana at Palmetto Bend Dam (USGS-08164525) GAM summary for TP.

Component	Term	Estimate	Std Error	t-value	p-value	
A. parametric coefficients	(Intercept)	-1.624	0.037	-44.377	0.0000	***
Component	**Term**	**edf**	**Ref. df**	**F-value**	**p-value**	
B. smooth terms	s(ddate)	3.214	8.000	1.862	0.0009	***
	s(yday)	1.309	8.000	0.374	0.0879	.
	s(log1p_inflow)	0.003	9.000	0.000	0.3600	
	s(log1p_Flow)	1.104	4.000	0.561	0.0982	.
	s(stfa)	0.000	5.000	0.000	0.4699	
	s(ma)	2.262	5.000	1.669	0.0060	**

Signif. codes: 0 <= '***' < 0.001 < '**' < 0.01 < '*' < 0.05

Adjusted R-squared: 0.321, Deviance explained 0.388

-REML : -99.963, Scale est: 0.00403, N: 81

Table 9. Navidad River at Strane Pk near Edna (USGS-08164390) GAM summary for NO_3.

Component	Term	Estimate	Std Error	t-value	p-value	
A. parametric coefficients	(Intercept)	-2.037	0.102	-20.057	0.0000	***
Component	**Term**	**edf**	**Ref. df**	**F-value**	**p-value**	
B. smooth terms	s(ddate)	1.685	17.000	0.781	0.0007	***
	s(yday)	2.486	4.000	5.143	0.0001	***
	s(log1p_Flow)	4.072	5.000	11.579	0.0000	***
	s(ma)	2.227	4.000	3.098	0.0010	**
	s(ltfa)	0.001	9.000	0.000	0.3874	

Signif. codes: 0 <= '***' < 0.001 < '**' < 0.01 < '*' < 0.05

Adjusted R-squared: 0.717, Deviance explained 0.767

-REML : -46.034, Scale est: 0.00733, N: 59

Table 10. Navidad River at Strane Pk near Edna (USGS-08164390) GAM summary for TP.

Component	Term	Estimate	Std Error	t-value	p-value	
A. parametric coefficients	(Intercept)	-1.567	0.034	-45.461	0.0000	***
Component	**Term**	**edf**	**Ref. df**	**F-value**	**p-value**	
B. smooth terms	s(ddate)	7.028	17.000	3.428	0.0000	***
	s(yday)	0.000	4.000	0.000	0.4175	
	s(log1p_Flow)	3.434	5.000	5.219	0.0000	***
	s(stfa)	0.000	5.000	0.000	0.8293	
	s(ma)	0.000	5.000	0.000	0.7003	

Signif. codes: 0 <= '***' < 0.001 < '**' < 0.01 < '*' < 0.05

Adjusted R-squared: 0.557, Deviance explained 0.617

-REML : -89.245, Scale est: 0.00359, N: 77

Table 11. Sandy Creek near Ganado (USGS-08164450) GAM summary for NO_3.

Component	Term	Estimate	Std Error	t-value	p-value	
A. parametric coefficients	(Intercept)	-2.172	0.118	-18.432	0.0000	***
Component	**Term**	**edf**	**Ref. df**	**F-value**	**p-value**	
B. smooth terms	s(ddate)	1.039	17.000	0.199	0.0324	*
	s(yday)	2.282	4.000	4.551	0.0002	***
	s(log1p_Flow)	3.542	5.000	2.555	0.0057	**
	s(ma)	4.307	5.000	4.620	0.0003	***
	s(ltfa)	4.222	5.000	6.270	0.0000	***

Signif. codes: 0 <= '***' < 0.001 < '**' < 0.01 < '*' < 0.05

Adjusted R-squared: 0.737, Deviance explained 0.810

-REML : -34.378, Scale est: 0.00738, N: 56

Table 12. Sandy Creek near Ganado (USGS-08164450) GAM summary for TP.

Component	Term	Estimate	Std Error	t-value	p-value	
A. parametric coefficients	(Intercept)	-1.729	0.067	-25.973	0.0000	***
Component	**Term**	**edf**	**Ref. df**	**F-value**	**p-value**	
B. smooth terms	s(ddate)	9.316	17.000	4.295	0.0000	***
	s(yday)	0.000	4.000	0.000	0.7298	
	s(log1p_Flow)	6.939	9.000	2.967	0.0003	***
	s(stfa)	2.097	5.000	0.757	0.0902	.
	s(ma)	2.171	4.000	3.529	0.0003	***

Signif. codes: 0 <= '***' < 0.001 < '**' < 0.01 < '*' < 0.05

Adjusted R-squared: 0.757, Deviance explained 0.824

-REML : -34.024, Scale est: 0.00944, N: 75

Table 13. East Mustang Creek near Louise (USGS-08164504) GAM summary for NO_3.

Component	Term	Estimate	Std Error	t-value	p-value	
A. parametric coefficients	(Intercept)	-1.124	0.226	-4.977	0.0000	***
Component	**Term**	**edf**	**Ref. df**	**F-value**	**p-value**	
B. smooth terms	s(ddate)	7.624	17.000	1.872	0.0000	***
	s(yday)	2.721	4.000	10.228	0.0000	***
	s(log1p_Flow)	3.734	4.000	18.724	0.0000	***
	s(ma)	2.170	5.000	1.213	0.0041	**
	s(ltfa)	4.770	9.000	1.982	0.0000	***

Signif. codes: 0 <= '***' < 0.001 < '**' < 0.01 < '*' < 0.05

Adjusted R-squared: 0.965, Deviance explained 0.977

-REML : 79.611, Scale est: 0.222, N: 61

Table 14. East Mustang Creek near Lousie (USGS-08164504) GAM summary for TP.

Component	Term	Estimate	Std Error	t-value	p-value	
A. parametric coefficients	(Intercept)	-0.961	0.083	-11.552	0.0000	***
Component	**Term**	**edf**	**Ref. df**	**F-value**	**p-value**	
B. smooth terms	s(ddate)	0.662	17.000	0.115	0.0857	.
	s(yday)	0.941	8.000	0.212	0.1565	
	s(log1p_Flow)	2.652	4.000	7.249	0.0000	***
	s(ma)	0.002	5.000	0.000	0.3785	
	s(stfa)	0.000	4.000	0.000	0.4802	

Signif. codes: 0 <= '***' < 0.001 < '**' < 0.01 < '*' < 0.05

Adjusted R-squared: 0.284, Deviance explained 0.323

-REML : 11.403, Scale est: 0.0685, N: 79

Table 15. West Mustang Creek near Ganado (USGS-08164503) GAM summary for NO_3.

Component	Term	Estimate	Std Error	t-value	p-value	
A. parametric coefficients	(Intercept)	-1.397	0.136	-10.240	0.0000	***
Component	**Term**	**edf**	**Ref. df**	**F-value**	**p-value**	
B. smooth terms	s(ddate)	1.200	17.000	0.160	0.0699	.
	s(yday)	2.756	4.000	13.576	0.0000	***
	s(log1p_Flow)	5.246	6.000	12.932	0.0000	***
	s(ma)	2.729	5.000	3.410	0.0002	***
	s(ltfa)	6.227	9.000	3.816	0.0000	***

Signif. codes: 0 <= '***' < 0.001 < '**' < 0.01 < '*' < 0.05

Adjusted R-squared: 0.873, Deviance explained 0.910

-REML : 19.712, Scale est: 0.0422, N: 63

Table 16. West Mustang Creek near Ganado (USGS-08164503) GAM summary for TP.

Component	Term	Estimate	Std Error	t-value	p-value	
A. parametric coefficients	(Intercept)	-1.226	0.065	-18.913	0.0000	***
Component	**Term**	**edf**	**Ref. df**	**F-value**	**p-value**	
B. smooth terms	s(ddate)	5.824	17.000	5.644	0.0000	***
	s(yday)	0.000	4.000	0.000	0.3905	
	s(log1p_Flow)	6.389	9.000	3.021	0.0002	***
	s(stfa)	2.722	5.000	1.042	0.0859	.
	s(ma)	0.000	5.000	0.000	0.4937	

Signif. codes: 0 <= '***' < 0.001 < '**' < 0.01 < '*' < 0.05

Adjusted R-squared: 0.487, Deviance explained 0.583

-REML : -10.462, Scale est: 0.0263, N: 81

Appendix B: Daily and Monthly Nutrient Loading

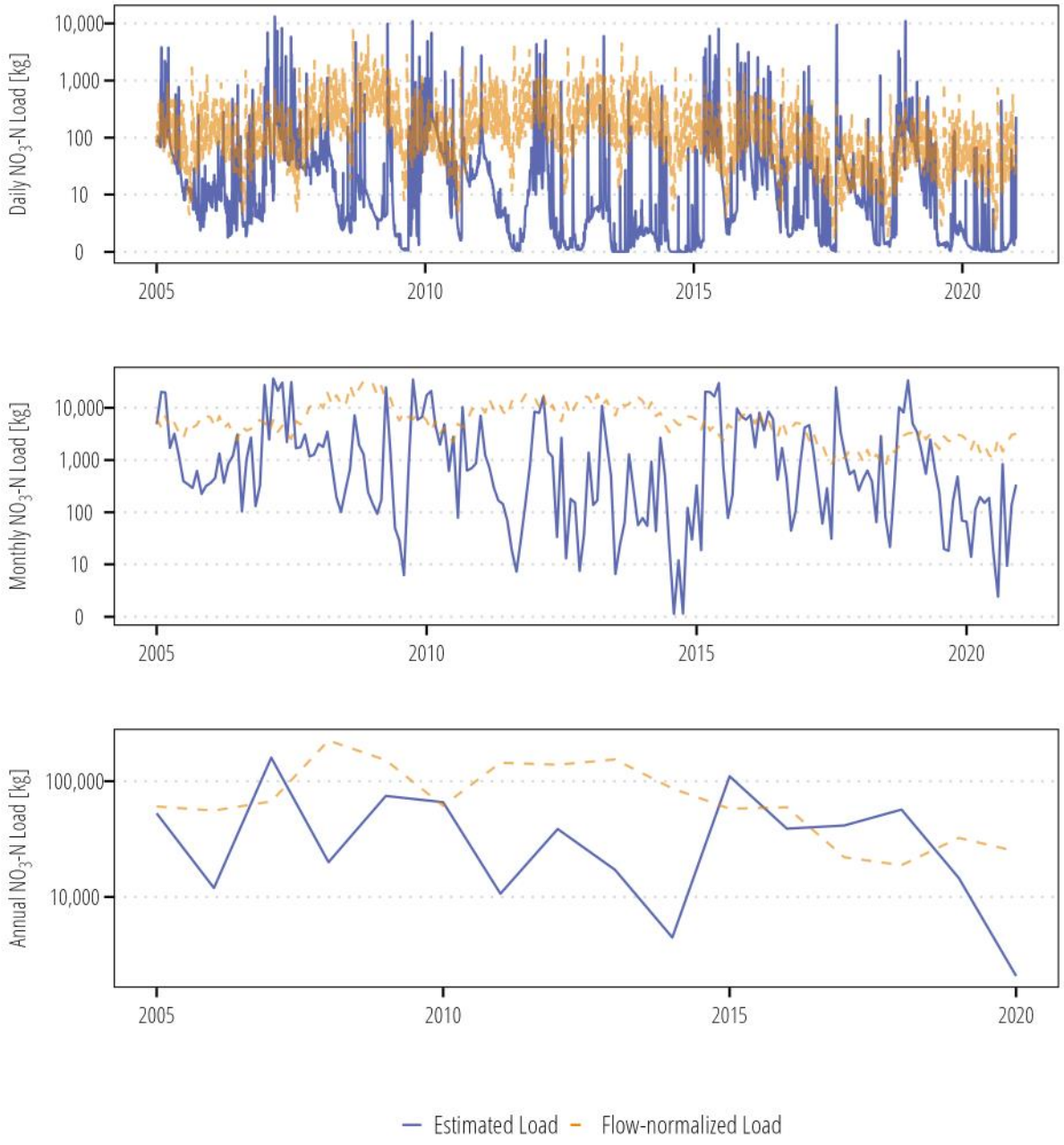

Figure 11. NO_3 loads at Lavaca River (USGS-08164000).

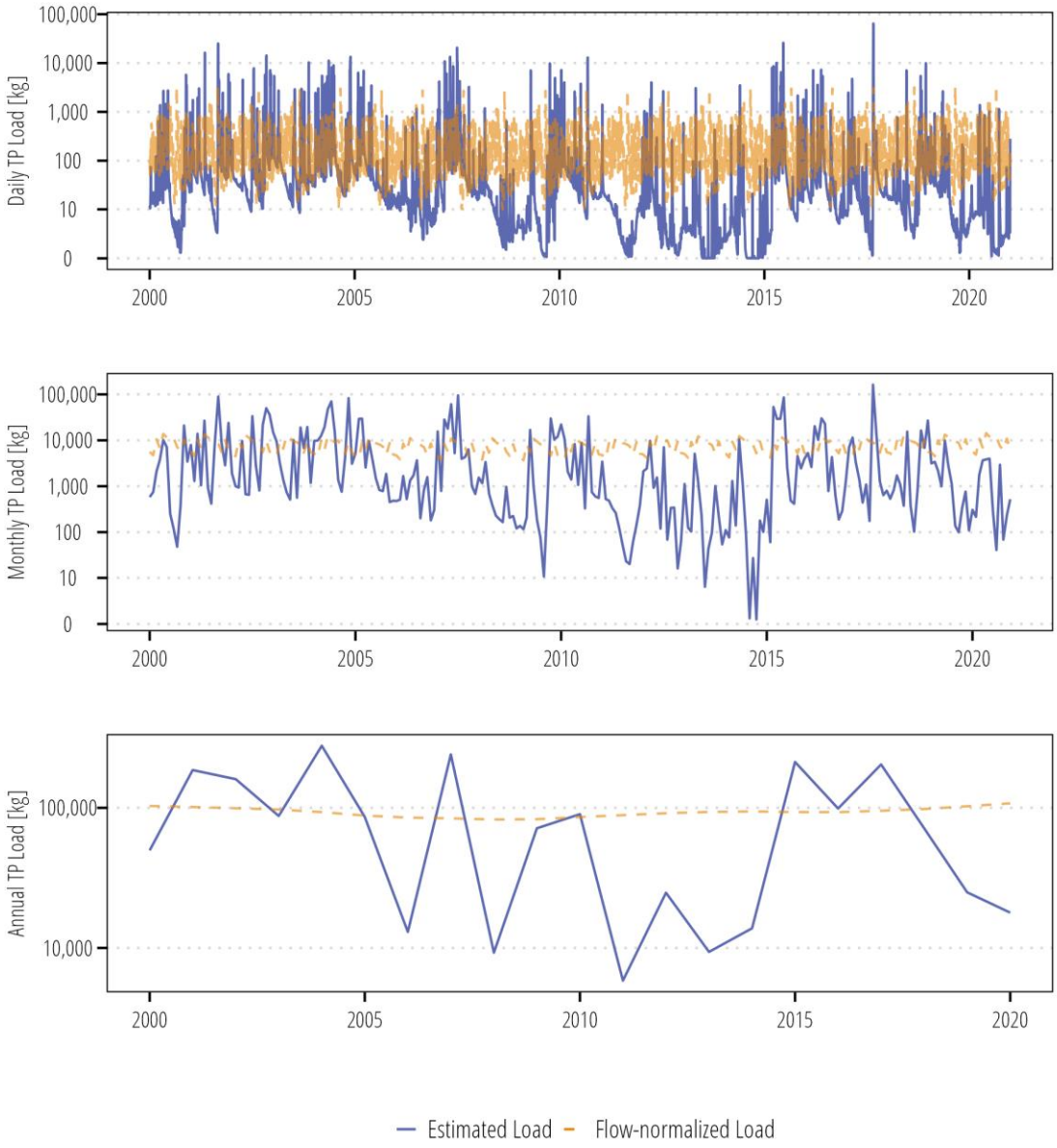

Figure 12. TP loads at Lavaca River (USGS-08164000).

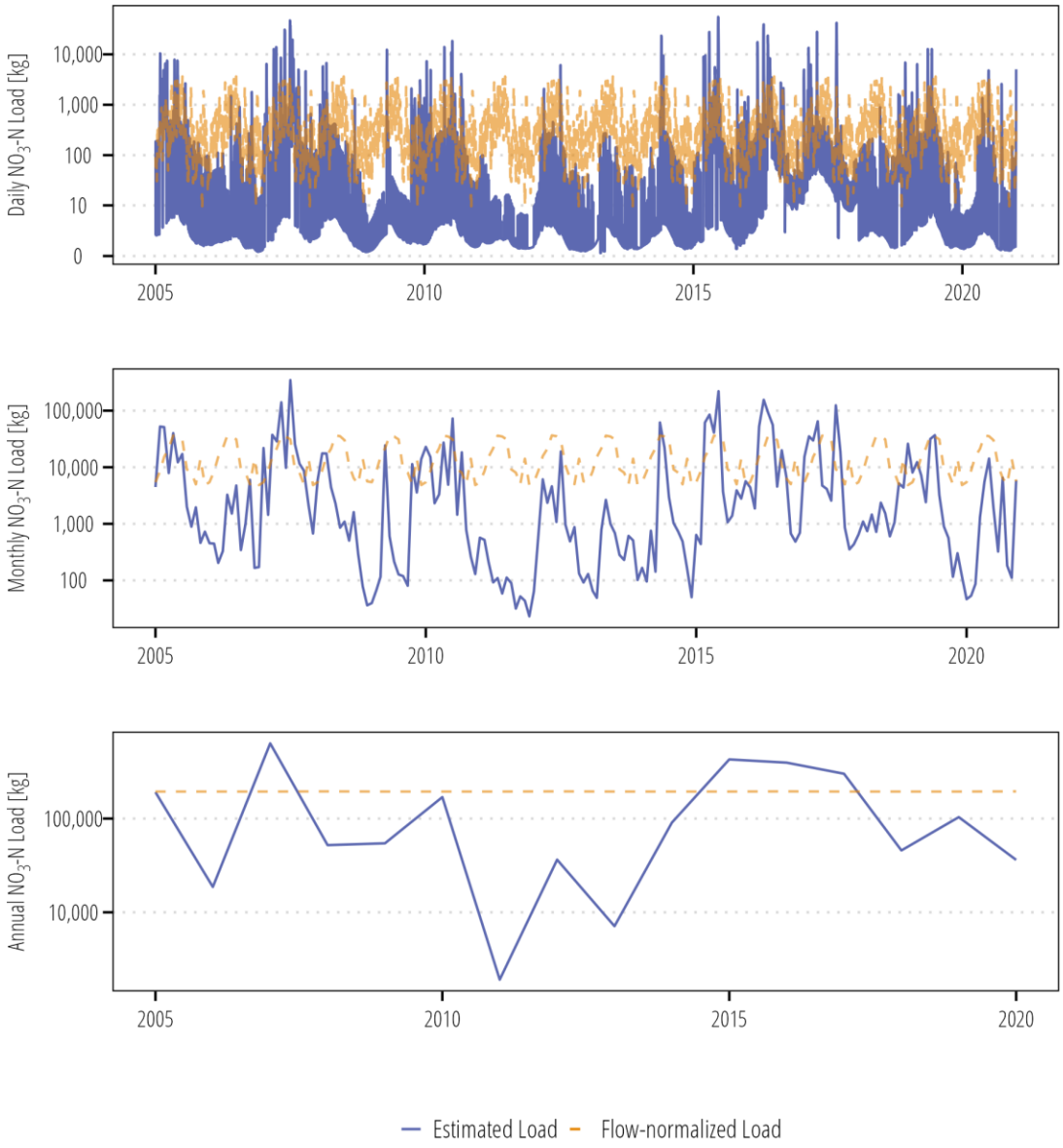

Figure 13. NO_3 loads at Navidad River (Lake Texana discharge; USGS-08164525).

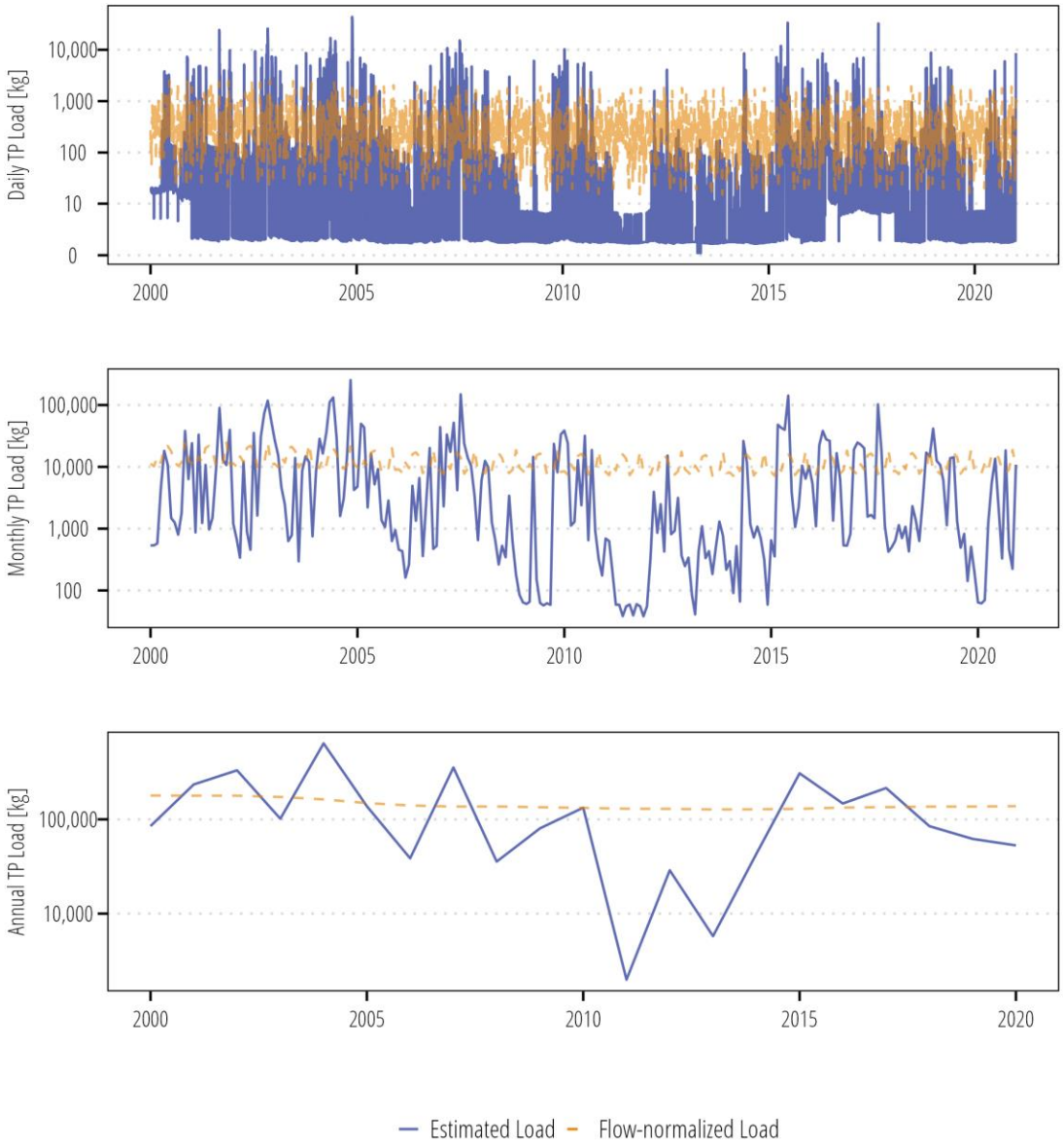

Figure 14. TP loads at Navidad River (Lake Texana discharge; USGS-08164525).

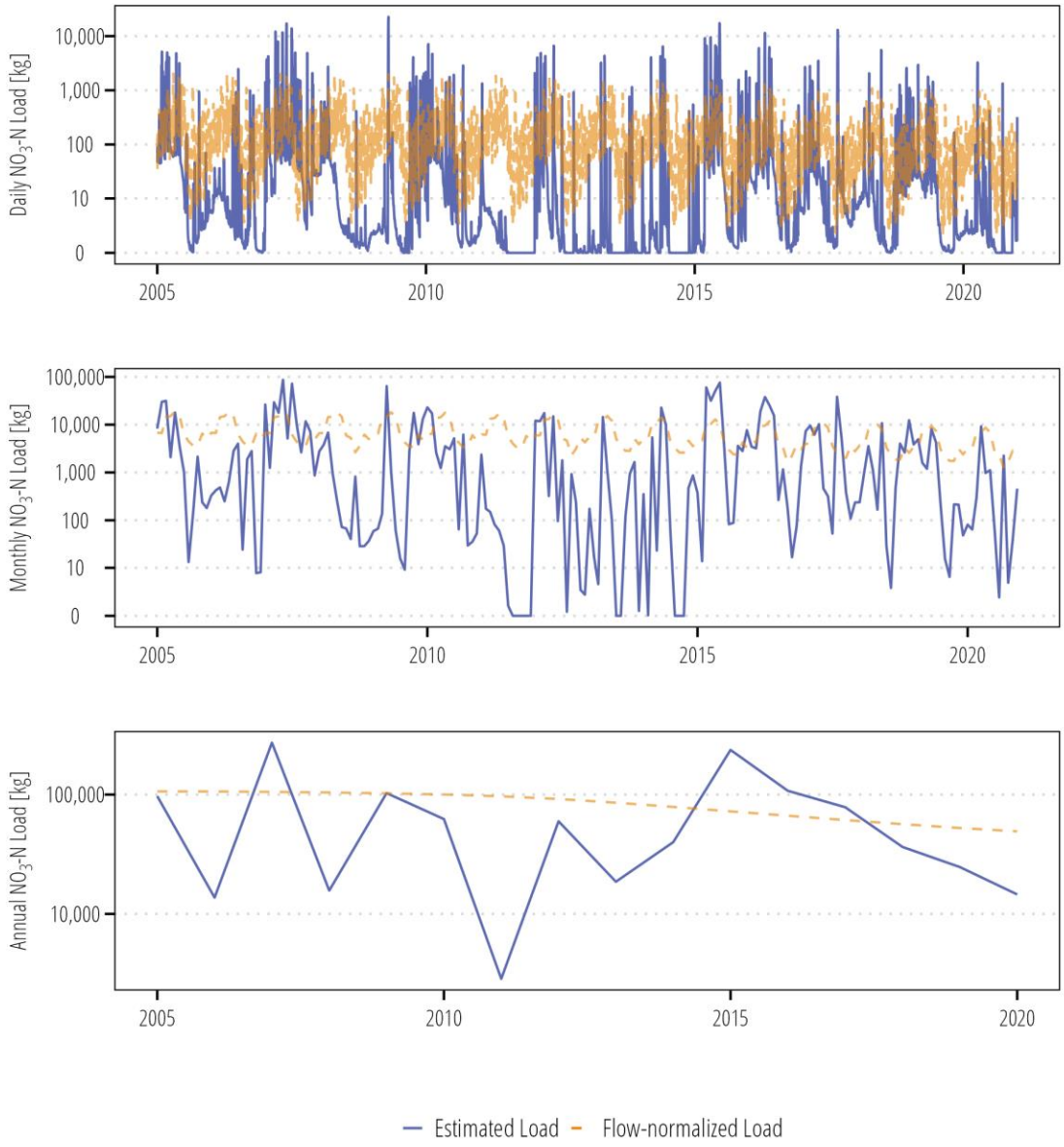

Figure 15. NO_3 loads at Navidad River at Strane Pk (USGS-08164390).

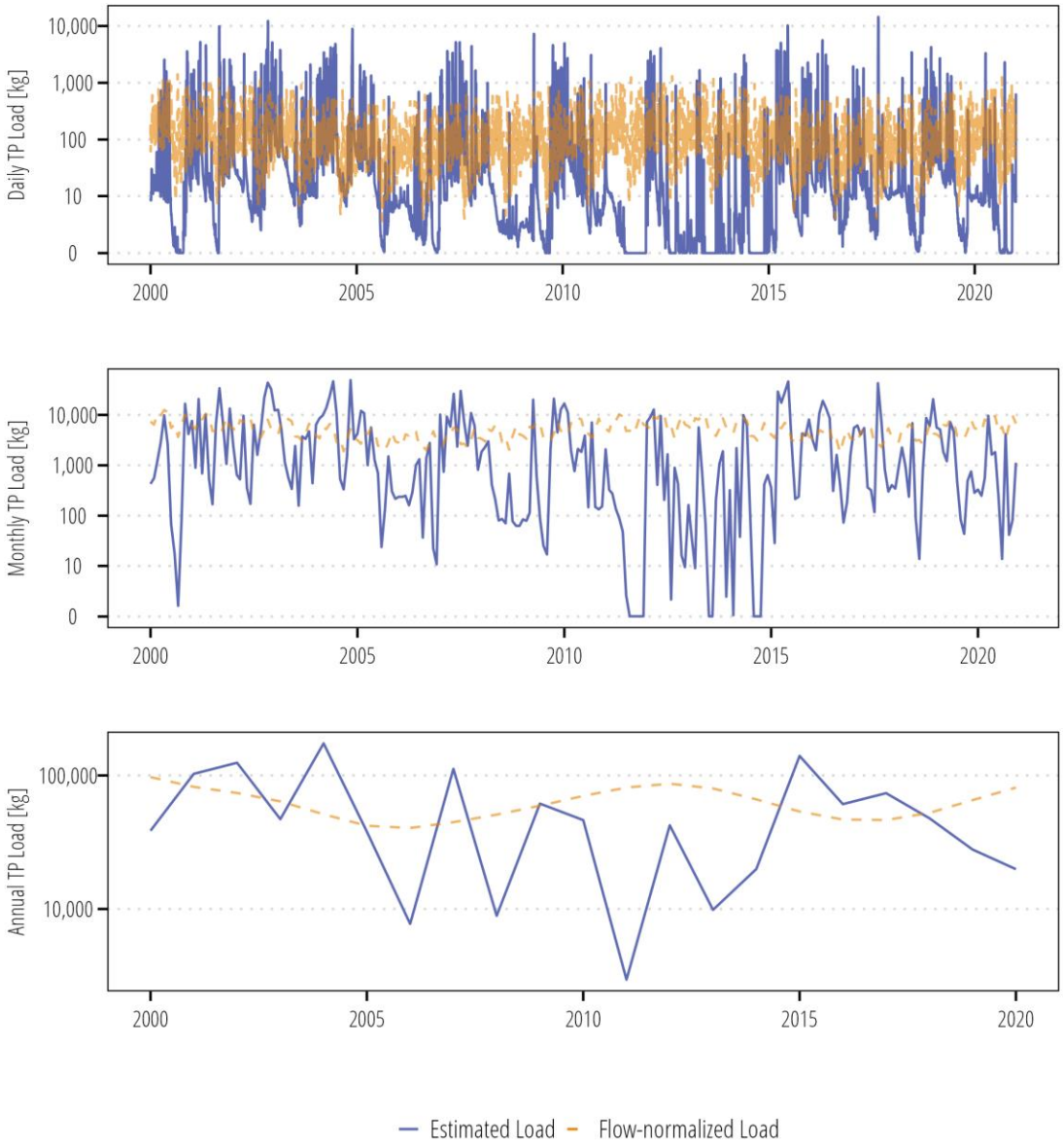

Figure 16. TP loads at Navidad River at Strane Pk (USGS-08164390).

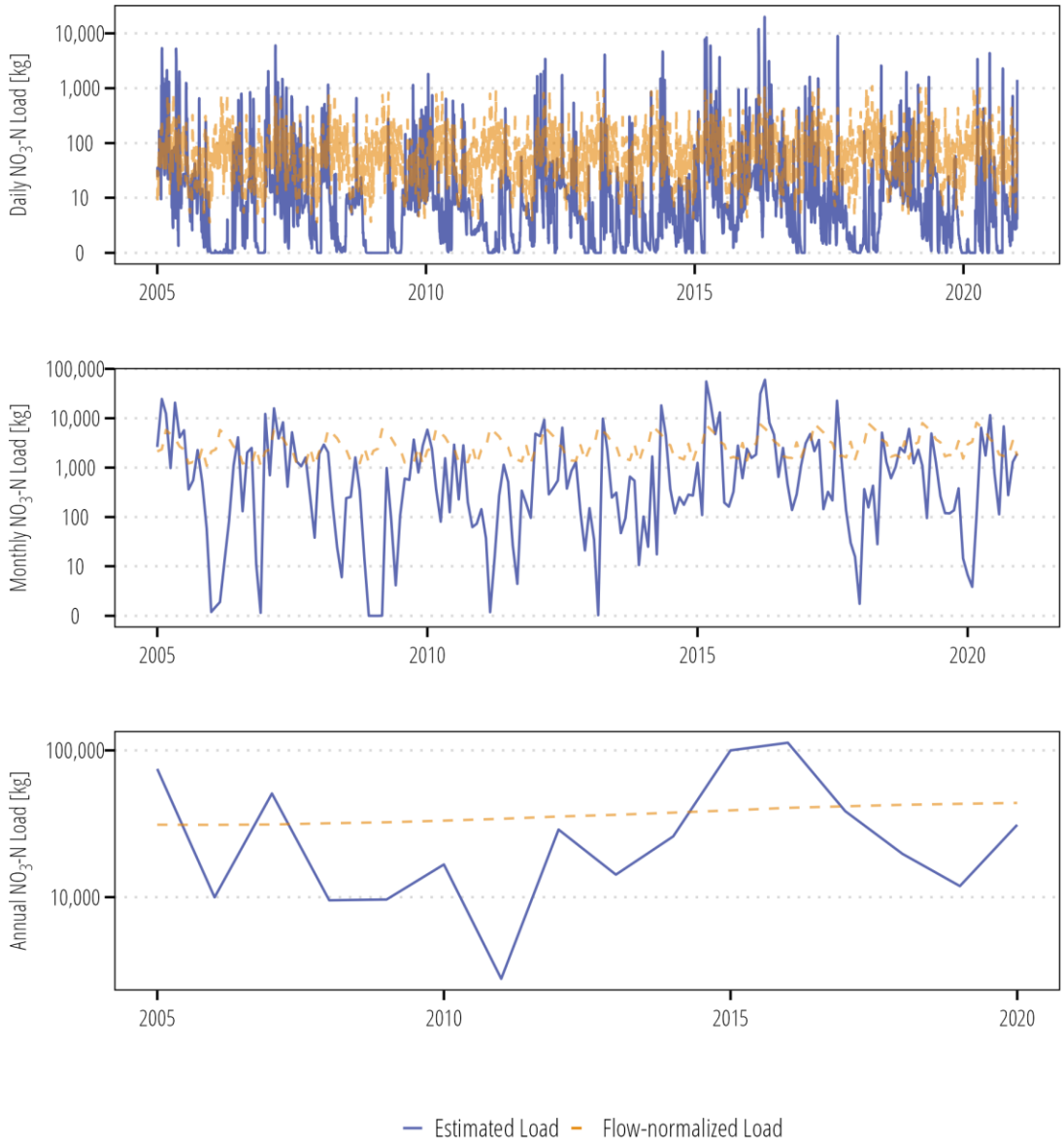

Figure 17. NO_3 loads at Sandy Creek (USGS-08164450).

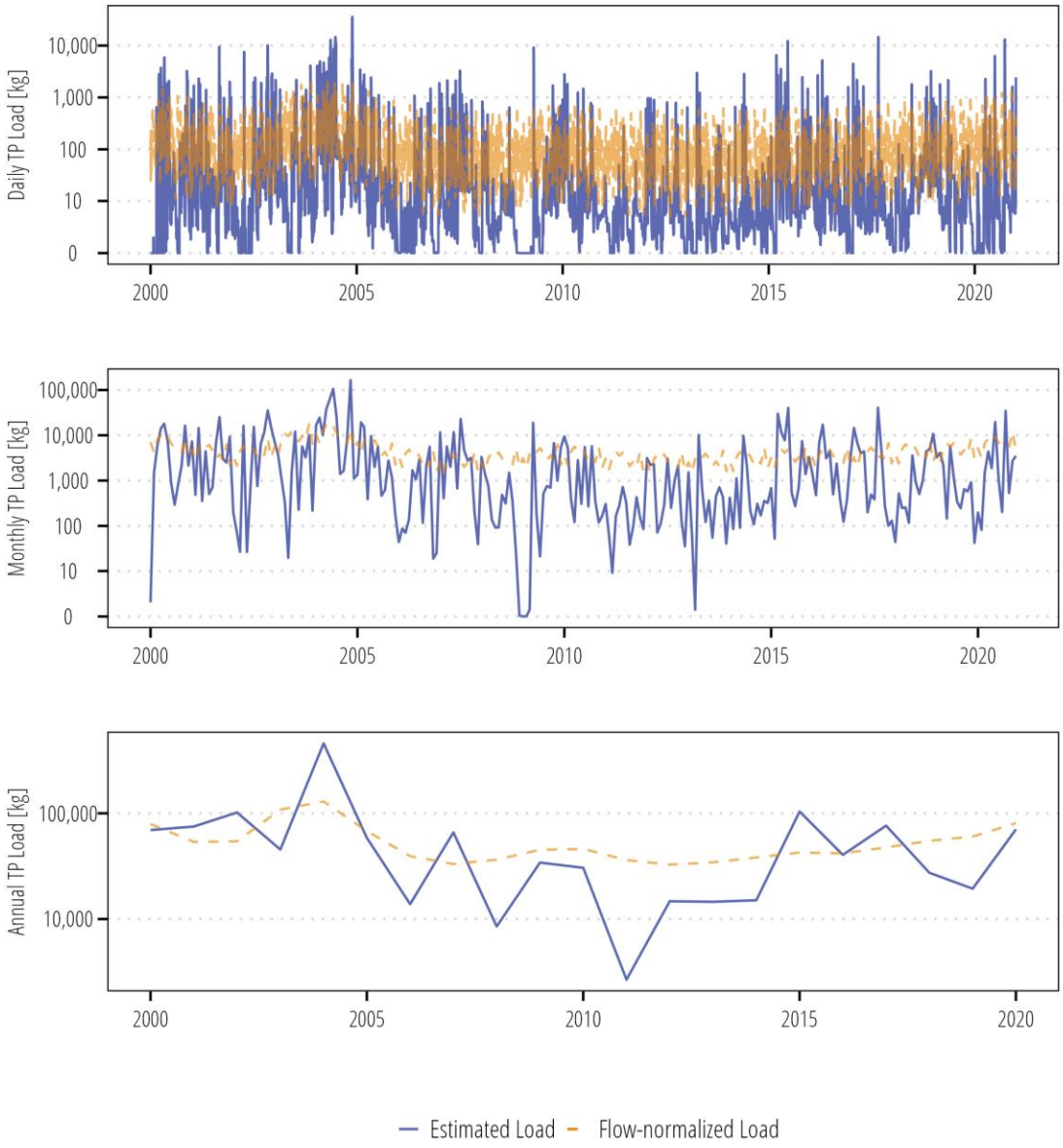

Figure 18. TP loads at Sandy Creek (USGS-08164450).

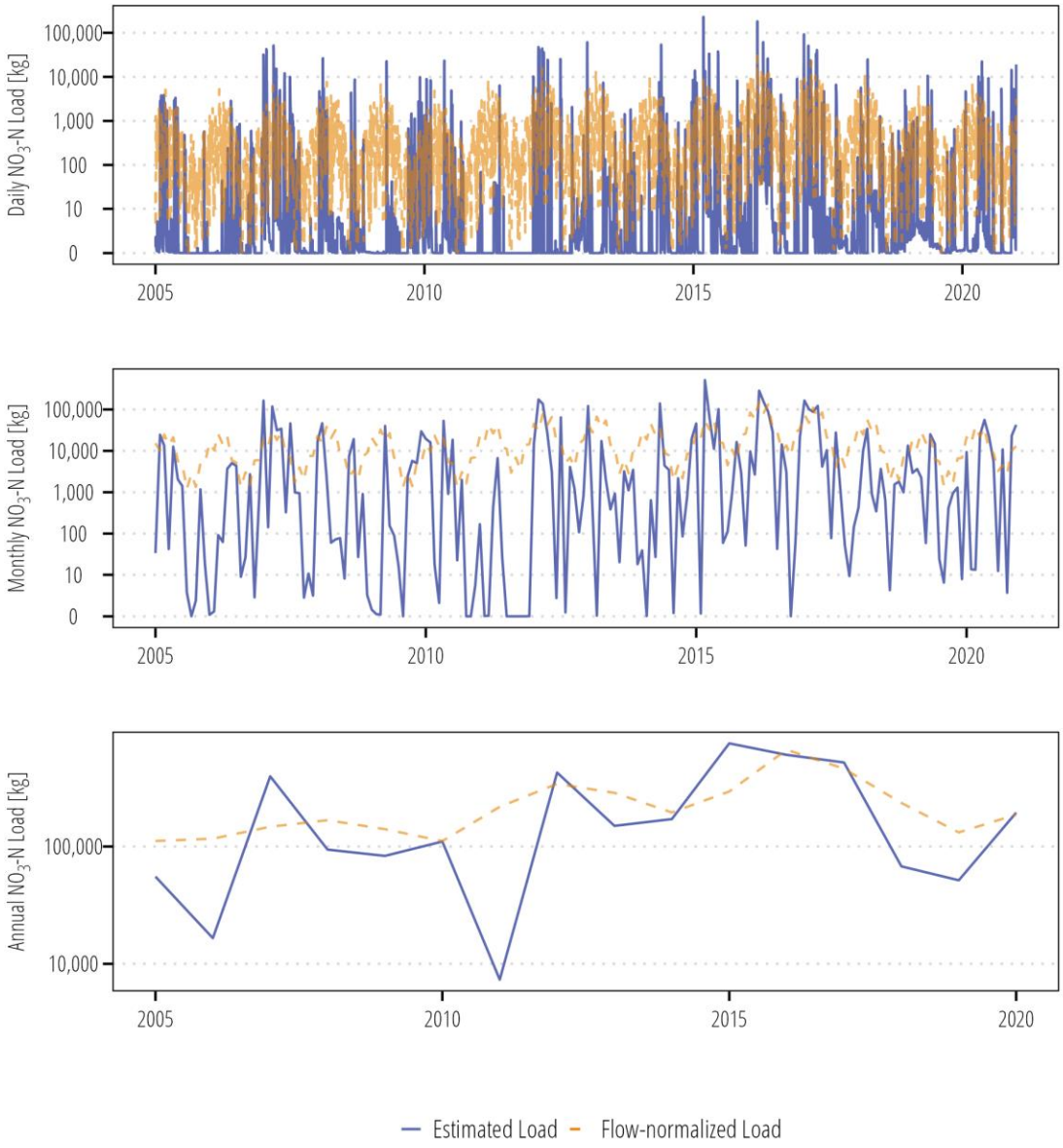

Figure 19. NO_3 loads at East Mustang Creek (USGS-08164504).

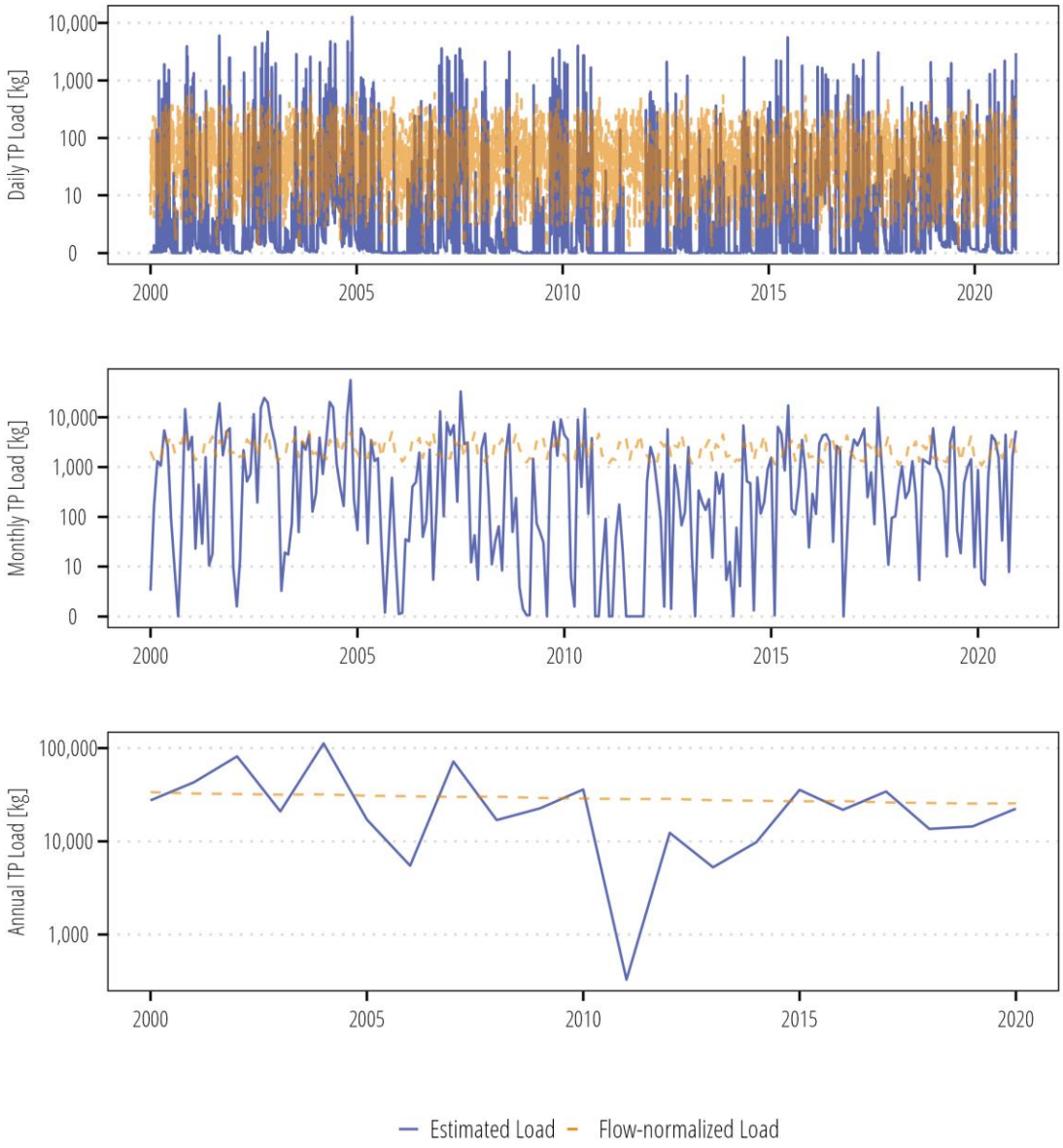

Figure 20. TP loads at East Mustang Creek (USGS-0816504).

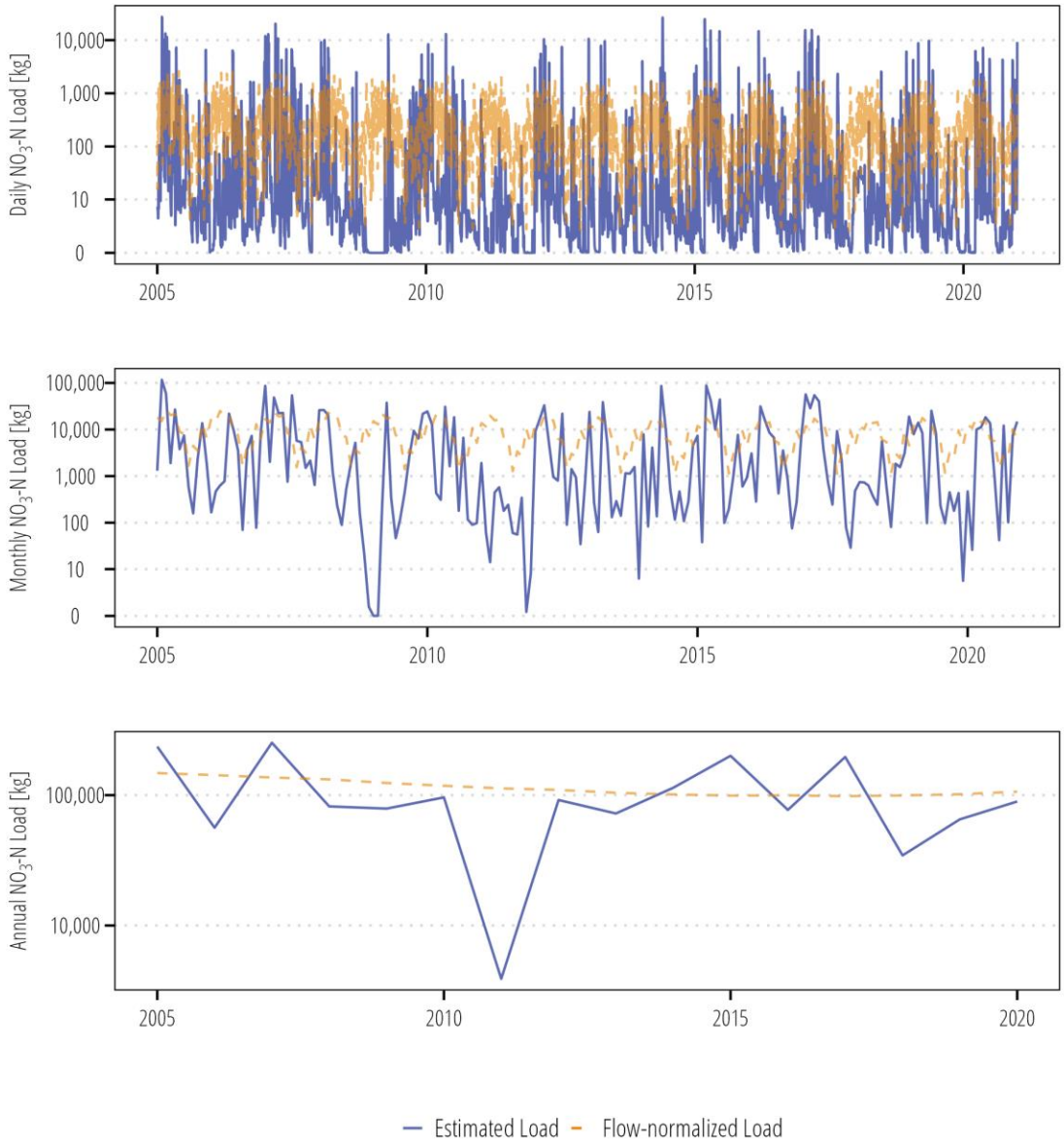

Figure 21. NO_3 loads at West Mustang Creek (USGS-08164503).

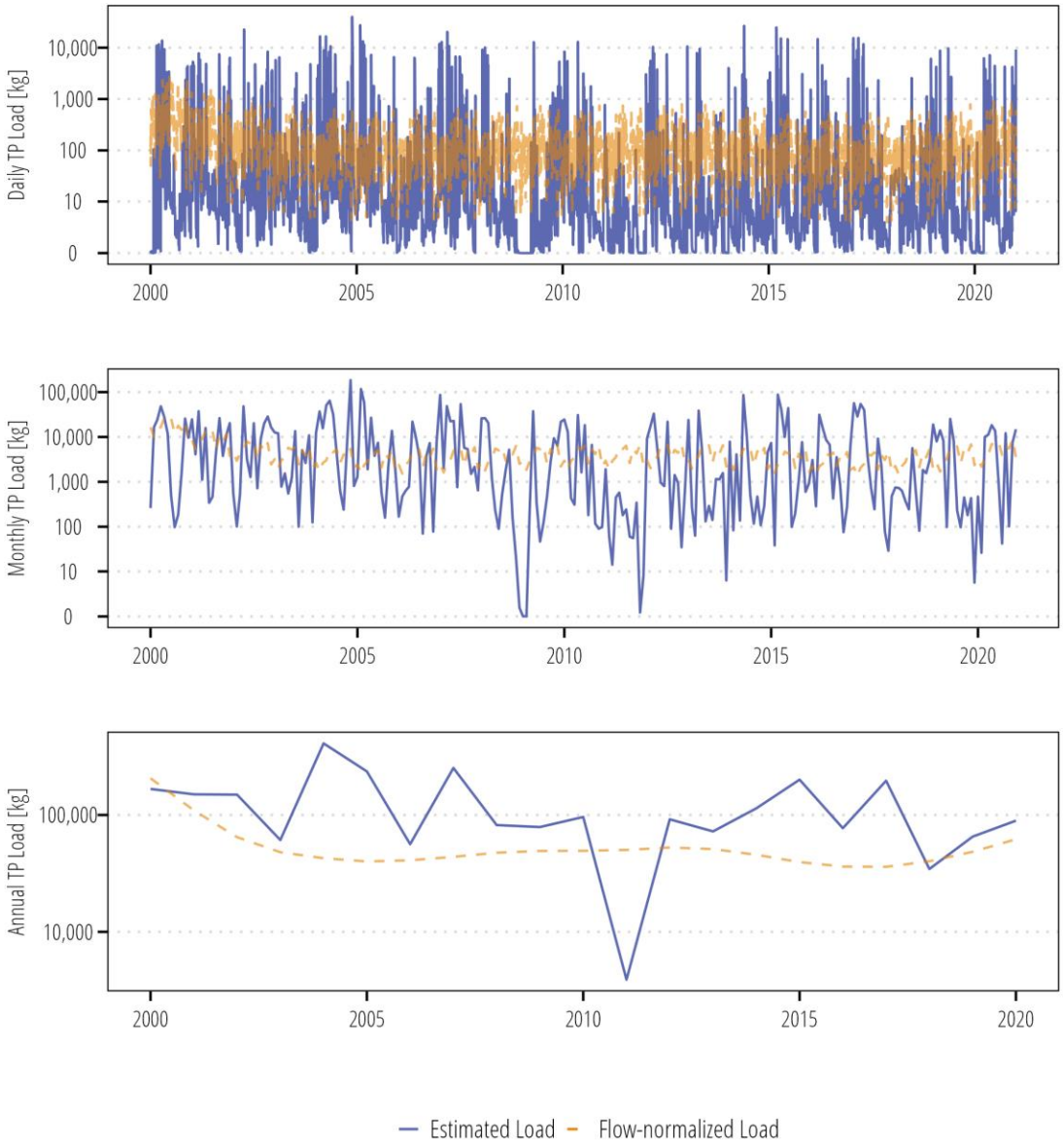

Figure 22. TP loads at West Mustang Creek (USGS-08164503).

Appendix C – Estuary GAM Model Summaries,

Total Phosphorus Models

Table 17. Temporal GAM summary for TP concentration at TCEQ-13563.

Component	Term	Estimate	Std Error	t-value	p-value	
A. parametric coefficients	(Intercept)	-2.052	0.065	-31.636	0.0000	***
Component	**Term**	**edf**	**Ref. df**	**F-value**	**p-value**	
B. smooth terms	s(day)	1.419	3.000	1.327	0.0642	.
	s(ddate)	0.000	19.000	0.000	0.5354	

Signif. codes: 0 <= '***' < 0.001 < '**' < 0.01 < '*' < 0.05

Adjusted R-squared: 0.071, Deviance explained 0.104

-REML : -73.311, Scale est: 0.210, N: 50

Table 18. Inflow GAM summary for TP concentration at TCEQ-13563.

Component	Term	Estimate	Std Error	t-value	p-value	
A. parametric coefficients	(Intercept)	-2.078	0.058	-35.901	0.0000	***
Component	**Term**	**edf**	**Ref. df**	**F-value**	**p-value**	
B. smooth terms	s(inflow)	2.186	7.000	2.184	0.0008	***
	s(day)	0.638	3.000	0.266	0.2885	
	s(ddate)	0.000	19.000	0.000	0.9722	

Signif. codes: 0 <= '***' < 0.001 < '**' < 0.01 < '*' < 0.05

Adjusted R-squared: 0.344, Deviance explained 0.347

-REML : -78.843, Scale est: 0.167, N: 50

Table 19. Inflow plus load GAM summary for TP concentration at TCEQ-13563.

Component	Term	Estimate	Std Error	t-value	p-value	
A. parametric coefficients	(Intercept)	-2.084	0.056	-37.418	0.0000	***
Component	**Term**	**edf**	**Ref. df**	**F-value**	**p-value**	
B. smooth terms	s(inflow)	2.183	7.000	2.074	0.0010	**
	s(TP load)	0.738	7.000	0.357	0.0665	.
	s(day)	1.130	3.000	0.707	0.1512	
	s(ddate)	0.000	19.000	0.000	0.9511	

Signif. codes: 0 <= '***' < 0.001 < '**' < 0.01 < '*' < 0.05

Adjusted R-squared: 0.378, Deviance explained 0.407

-REML : -79.480, Scale est: 0.155, N: 50

Table 20. Temporal GAM summary for TP concentration at TCEQ-13383.

Component	**Term**	**Estimate**	**Std Error**	**t-value**	**p-value**	
A. parametric coefficients	(Intercept)	-2.252	0.066	-34.284	0.0000	***
Component	**Term**	**edf**	**Ref. df**	**F-value**	**p-value**	
B. smooth terms	s(day)	1.835	3.000	3.349	0.0052	**
	s(ddate)	0.000	19.000	0.000	0.7181	

Signif. codes: 0 <= '***' < 0.001 < '**' < 0.01 < '*' < 0.05

Adjusted R-squared: 0.163, Deviance explained 0.209

-REML : -76.343, Scale est: 0.203, N: 47

Table 21. Inflow GAM summary for TP concentration at TCEQ-13383.

Component	Term	Estimate	Std Error	t-value	p-value	
A. parametric coefficients	(Intercept)	-2.264	0.063	-35.666	0.0000	***
Component	**Term**	**edf**	**Ref. df**	**F-value**	**p-value**	
B. smooth terms	s(inflow)	0.846	7.000	0.765	0.0146	*
	s(day)	1.662	3.000	2.213	0.0204	*
	s(ddate)	0.000	19.000	0.000	0.9560	

Signif. codes: 0 <= '***' < 0.001 < '**' < 0.01 < '*' < 0.05

Adjusted R-squared: 0.257, Deviance explained 0.302

-REML : -78.284, Scale est: 0.189, N: 47

Table 22. Inflow plus load GAM summary for TP concentration at TCEQ-13383.

Component	Term	Estimate	Std Error	t-value	p-value	
A. parametric coefficients	(Intercept)	-2.273	0.059	-38.421	0.0000	***
Component	**Term**	**edf**	**Ref. df**	**F-value**	**p-value**	
B. smooth terms	s(inflow)	0.843	7.000	0.791	0.0130	*
	s(TP load)	0.771	7.000	0.504	0.0350	*
	s(day)	1.840	3.000	3.291	0.0054	**
	s(ddate)	0.000	19.000	0.000	0.8997	

Signif. codes: 0 <= '***' < 0.001 < '**' < 0.01 < '*' < 0.05

Adjusted R-squared: 0.334, Deviance explained 0.372

-REML : -79.145, Scale est: 0.164, N: 47

Table 23. Temporal GAM summary for TP concentration at TCEQ-13384.

Component	Term	Estimate	Std Error	t-value	p-value	
A. parametric coefficients	(Intercept)	-2.563	0.061	-42.167	0.0000	***
Component	**Term**	**edf**	**Ref. df**	**F-value**	**p-value**	
B. smooth terms	s(day)	0.634	3.000	0.345	0.2011	
	s(ddate)	0.895	19.000	0.129	0.0739	.

Signif. codes: 0 <= '***' < 0.001 < '**' < 0.01 < '*' < 0.05

Adjusted R-squared: 0.0664, Deviance explained 0.0839

-REML : -98.633, Scale est: 0.188, N: 51

Table 24. Inflow GAM summary for TP concentration at TCEQ-13384.

Component	Term	Estimate	Std Error	t-value	p-value	
A. parametric coefficients	(Intercept)	-2.577	0.058	-44.244	0.0000	***
Component	**Term**	**edf**	**Ref. df**	**F-value**	**p-value**	
B. smooth terms	s(inflow)	1.772	7.000	1.130	0.0121	*
	s(day)	0.000	3.000	0.000	0.3897	
	s(ddate)	0.814	19.000	0.256	0.0180	*

Signif. codes: 0 <= '***' < 0.001 < '**' < 0.01 < '*' < 0.05

Adjusted R-squared: 0.192, Deviance explained 0.210

-REML : -100.336, Scale est: 0.173, N: 51

Table 25. Inflow plus load GAM summary for TP concentration at TCEQ-13384.

Component	Term	Estimate	Std Error	t-value	p-value	
A. parametric coefficients	(Intercept)	-2.577	0.058	-44.244	0.0000	***
Component	**Term**	**edf**	**Ref. df**	**F-value**	**p-value**	
B. smooth terms	s(inflow)	1.772	7.000	1.130	0.0121	*
	s(TP load)	0.000	7.000	0.000	0.3461	
	s(day)	0.000	3.000	0.000	0.3897	
	s(ddate)	0.814	19.000	0.256	0.0180	*

Signif. codes: 0 <= '***' < 0.001 < '**' < 0.01 < '*' < 0.05

Adjusted R-squared: 0.192, Deviance explained 0.210

-REML : -100.336, Scale est: 0.173, N: 51

Nitrite+Nitrate Models

Table 26. Temporal GAM summary for NO_x concentration at TCEQ-13563.

Component	**Term**	**Estimate**	**Std Error**	**t-value**	**p-value**	
A. parametric coefficients	(Intercept)	-2.772	0.156	-17.805	0.0000	***
Component	**Term**	**edf**	**Ref. df**	**F-value**	**p-value**	
B. smooth terms	s(day)	2.400	4.000	3.617	0.0014	**
	s(ddate)	0.911	8.000	0.637	0.0200	*

Signif. codes: 0 <= '***' < 0.001 < '**' < 0.01 < '*' < 0.05

Adjusted R-squared: 0.155, Deviance explained 0.352

-REML : -87.865, Scale est: 1.284, N: 53

Table 27. Inflow GAM summary for NO_x concentration at TCEQ-13563

Component	**Term**	**Estimate**	**Std Error**	**t-value**	**p-value**	
A. parametric coefficients	(Intercept)	-2.901	0.136	-21.388	0.0000	***
Component	**Term**	**edf**	**Ref. df**	**F-value**	**p-value**	
B. smooth terms	s(inflow)	1.034	6.000	2.036	0.0007	***
	s(day)	2.458	4.000	3.125	0.0036	**
	s(ddate)	0.724	8.000	0.208	0.1330	

Signif. codes: 0 <= '***' < 0.001 < '**' < 0.01 < '*' < 0.05

Adjusted R-squared: 0.459, Deviance explained 0.527

-REML : -95.240, Scale est: 0.975, N: 53

Table 28. Inflow plus load GAM summary for NO_x concentration at TCEQ-13563.

Component	Term	Estimate	Std Error	t-value	p-value	
A. parametric coefficients	(Intercept)	-2.901	0.136	-21.388	0.0000	
Component	**Term**	**edf**	**Ref. df**	**F-value**	**p-value**	
B. smooth terms	s(inflow)	1.034	6.000	2.036	0.0007	
	s(NO_3-N load)	0.000	7.000	0.000	0.4168	
	s(day)	2.458	4.000	3.125	0.0036	**
	s(ddate)	0.724	8.000	0.208	0.1330	

Signif. codes: 0 <= '***' < 0.001 < '**' < 0.01 < '*' < 0.05

Adjusted R-squared: 0.459, Deviance explained 0.527

-REML : -95.240, Scale est: 0.975, N: 53

Table 29. Temporal GAM summary for NO_x concentration at TCEQ-13383.

Component	**Term**	**Estimate**	**Std Error**	**t-value**	**p-value**	
A. parametric coefficients	(Intercept)	-3.314	0.154	-21.459	0.0000	***
Component	**Term**	**edf**	**Ref. df**	**F-value**	**p-value**	
B. smooth terms	s(day)	1.878	4.000	0.972	0.1172	
	s(ddate)	5.328	8.000	2.028	0.0122	*

Signif. codes: 0 <= '***' < 0.001 < '**' < 0.01 < '*' < 0.05

Adjusted R-squared: 0.130, Deviance explained 0.594

-REML : -104.729, Scale est: 1.216, N: 51

Table 30. Inflow GAM summary for NO_x concentration at TCEQ-13383.

Component	Term	Estimate	Std Error	t-value	p-value	
A. parametric coefficients	(Intercept)	-3.395	0.114	-29.685	0.0000	***
Component	**Term**	**edf**	**Ref. df**	**F-value**	**p-value**	
B. smooth terms	s(inflow)	1.700	6.000	5.631	0.0000	***
	s(day)	2.103	4.000	1.627	0.0359	*
	s(ddate)	0.535	8.000	0.092	0.2407	

Signif. codes: 0 <= '***' < 0.001 < '**' < 0.01 < '*' < 0.05

Adjusted R-squared: 0.356, Deviance explained 0.706

-REML : -122.152, Scale est: 0.667, N: 51

Table 31. Inflow plus load GAM summary for NO_x concentration at TCEQ-13383.

Component	Term	Estimate	Std Error	t-value	p-value
A. parametric coefficients	(Intercept)	-3.395	0.114	-29.685	0.0000
Component	**Term**	**edf**	**Ref. df**	**F-value**	**p-value**
B. smooth terms	s(inflow)	1.700	6.000	5.631	0.0000
	s(NO_3-N load)	0.000	7.000	0.000	0.7255
	s(day)	2.103	4.000	1.627	0.0359
	s(ddate)	0.535	8.000	0.092	0.2407

Signif. codes: 0 <= '***' < 0.001 < '**' < 0.01 < '*' < 0.05

Adjusted R-squared: 0.356, Deviance explained 0.706

-REML : -122.152, Scale est: 0.667, N: 51

Table 32. Temporal GAM summary for NO_x concentration at TCEQ-13384.

Component	**Term**	**Estimate**	**Std Error**	**t-value**	**p-value**	
A. parametric coefficients	(Intercept)	-3.515	0.143	-24.641	0.0000	***
Component	**Term**	**edf**	**Ref. df**	**F-value**	**p-value**	
B. smooth terms	s(day)	3.476	4.000	4.258	0.0024	**
	s(ddate)	0.000	8.000	0.000	0.6599	

Signif. codes: 0 <= '***' < 0.001 < '**' < 0.01 < '*' < 0.05

Adjusted R-squared: 0.0626, Deviance explained 0.494

-REML : -129.606, Scale est: 1.058, N: 52

Table 33. Inflow GAM summary for NO_x concentration at TCEQ-13384.

Component	**Term**	**Estimate**	**Std Error**	**t-value**	**p-value**	
A. parametric coefficients	(Intercept)	-3.667	0.069	-53.529	0.0000	***
Component	**Term**	**edf**	**Ref. df**	**F-value**	**p-value**	
B. smooth terms	s(inflow)	2.947	6.000	10.531	0.0000	***
	s(day)	2.113	4.000	2.318	0.0085	**
	s(ddate)	0.001	8.000	0.000	0.4346	

Signif. codes: 0 <= '***' < 0.001 < '**' < 0.01 < '*' < 0.05

Adjusted R-squared: 0.650, Deviance explained 0.813

-REML : -152.911, Scale est: 0.244, N: 52

Table 34. Inflow plus load GAM summary for NO_x concentration at TCEQ-13384.

Component	Term	Estimate	Std Error	t-value	p-value	
A. parametric coefficients	(Intercept)	-3.673	0.066	-55.273	0.0000	
Component	**Term**	**edf**	**Ref. df**	**F-value**	**p-value**	
B. smooth terms	s(inflow)	3.024	6.000	10.621	0.0000	
	s(NO_3-N load)	0.791	7.000	0.395	0.0613	.
	s(day)	2.013	4.000	1.948	0.0152	
	s(ddate)	0.000	8.000	0.000	0.5535	

Signif. codes: 0 <= '***' < 0.001 < '**' < 0.01 < '*' < 0.05

Adjusted R-squared: 0.664, Deviance explained 0.826

-REML : -153.724, Scale est: 0.230, N: 52

Chlorophyll-*a* Models

Table 35. Temporal GAM summary for chlorophyll-*a* concentration at TCEQ-13563.

Component	Term	Estimate	Std Error	t-value	p-value	
A. parametric coefficients	(Intercept)	2.223	0.070	31.640	0.0000	***
Component	**Term**	**edf**	**Ref. df**	**F-value**	**p-value**	
B. smooth terms	s(day)	1.540	3.000	1.874	0.0292	*
	s(ddate)	1.857	19.000	0.421	0.0135	*

Signif. codes: 0 <= '***' < 0.001 < '**' < 0.01 < '*' < 0.05

Adjusted R-squared: 0.191, Deviance explained 0.274

-REML : 143.945, Scale est: 0.242, N: 49

Table 36. Inflow GAM summary for chlorophyll-*a* concentration at TCEQ-13563.

Component	Term	Estimate	Std Error	t-value	p-value	
A. parametric coefficients	(Intercept)	2.204	0.064	34.186	0.0000	***
Component	**Term**	**edf**	**Ref. df**	**F-value**	**p-value**	
B. smooth terms	s(inflow)	1.721	7.000	1.153	0.0092	**
	s(day)	1.413	3.000	1.401	0.0534	.
	s(ddate)	1.867	19.000	0.573	0.0032	**

Signif. codes: 0 <= '***' < 0.001 < '**' < 0.01 < '*' < 0.05

Adjusted R-squared: 0.336, Deviance explained 0.401

-REML : 141.519, Scale est: 0.204, N: 49

Table 37. Inflow plus load GAM summary for chlorophyll-*a* concentration at TCEQ-13563.

Component	Term	Estimate	Std Error	t-value	p-value	
A. parametric coefficients	(Intercept)	2.204	0.064	34.186	0.0000	
Component	**Term**	**edf**	**Ref. df**	**F-value**	**p-value**	
B. smooth terms	s(inflow)	1.721	7.000	1.153	0.0092	**
	s(NO_3-N load)	0.000	7.000	0.000	0.6622	
	s(TP load)	0.000	7.000	0.000	0.9689	
	s(day)	1.413	3.000	1.401	0.0534	.
	s(ddate)	1.867	19.000	0.573	0.0032	**

Signif. codes: 0 <= '***' < 0.001 < '**' < 0.01 < '*' < 0.05

Adjusted R-squared: 0.336, Deviance explained 0.401

-REML : 141.519, Scale est: 0.204, N: 49

Table 38. Temporal GAM summary for chlorophyll-*a* concentration at TCEQ-13383

Component	**Term**	**Estimate**	**Std Error**	**t-value**	**p-value**	
A. parametric coefficients	(Intercept)	2.221	0.086	25.913	0.0000	***
Component	**Term**	**edf**	**Ref. df**	**F-value**	**p-value**	
B. smooth terms	s(day)	1.463	3.000	1.362	0.0662	.
	s(ddate)	0.000	19.000	0.000	0.4683	

Signif. codes: 0 <= '***' < 0.001 < '**' < 0.01 < '*' < 0.05

Adjusted R-squared: 0.0856, Deviance explained 0.121

-REML : 139.015, Scale est: 0.345, N: 47

Table 39. Inflow GAM summary for chlorophyll-*a* concentration at TCEQ-13383

Component	**Term**	**Estimate**	**Std Error**	**t-value**	**p-value**	
A. parametric coefficients	(Intercept)	2.211	0.082	26.819	0.0000	***
Component	**Term**	**edf**	**Ref. df**	**F-value**	**p-value**	
B. smooth terms	s(inflow)	0.777	7.000	0.405	0.0602	.
	s(day)	1.274	3.000	0.914	0.1211	
	s(ddate)	0.000	19.000	0.000	0.5367	

Signif. codes: 0 <= '***' < 0.001 < '**' < 0.01 < '*' < 0.05

Adjusted R-squared: 0.153, Deviance explained 0.183

-REML : 138.076, Scale est: 0.320, N: 47

Table 40. Inflow plus load GAM summary for chlorophyll-*a* concentration at TCEQ-13383

Component	**Term**	**Estimate**	**Std Error**	**t-value**	**p-value**	
A. parametric coefficients	(Intercept)	2.211	0.082	26.819	0.0000	
Component	**Term**	**edf**	**Ref. df**	**F-value**	**p-value**	
B. smooth terms	s(inflow)	0.777	7.000	0.405	0.0602	.
	s(NO_3-N load)	0.000	7.000	0.000	0.6871	
	s(TP load)	0.000	7.000	0.000	0.8833	
	s(day)	1.274	3.000	0.914	0.1211	
	s(ddate)	0.000	19.000	0.000	0.5371	

Signif. codes: 0 <= '***' < 0.001 < '**' < 0.01 < '*' < 0.05

Adjusted R-squared: 0.153, Deviance explained 0.183

-REML : 138.076, Scale est: 0.320, N: 47

Table 41. Temporal GAM summary for chlorophyll-*a* concentration at TCEQ-13384

Component	**Term**	**Estimate**	**Std Error**	**t-value**	**p-value**	
A. parametric coefficients	(Intercept)	2.032	0.088	22.968	0.0000	***
Component	**Term**	**edf**	**Ref. df**	**F-value**	**p-value**	
B. smooth terms	s(day)	2.583	3.000	4.373	0.0047	**
	s(ddate)	0.701	19.000	0.053	0.2400	

Signif. codes: 0 <= '***' < 0.001 < '**' < 0.01 < '*' < 0.05

Adjusted R-squared: 0.155, Deviance explained 0.285

-REML : 134.757, Scale est: 0.360, N: 46

Table 42. Inflow GAM summary for chlorophyll-a concentration at TCEQ-13384

Component	Term	Estimate	Std Error	t-value	p-value	
A. parametric coefficients	(Intercept)	2.032	0.088	22.967	0.0000	***
Component	**Term**	**edf**	**Ref. df**	**F-value**	**p-value**	
B. smooth terms	s(inflow)	0.000	7.000	0.000	0.7248	
	s(day)	2.583	3.000	4.372	0.0047	**
	s(ddate)	0.700	19.000	0.052	0.2401	

Signif. codes: 0 <= '***' < 0.001 < '**' < 0.01 < '*' < 0.05

Adjusted R-squared: 0.155, Deviance explained 0.285

-REML : 134.757, Scale est: 0.360, N: 46

Table 43. Inflow plus load GAM summary for chlorophyll-*a* concentration at TCEQ-13384

Component	**Term**	**Estimate**	**Std Error**	**t-value**	**p-value**	
A. parametric coefficients	(Intercept)	2.032	0.088	22.967	0.0000	
Component	**Term**	**edf**	**Ref. df**	**F-value**	**p-value**	
B. smooth terms	s(inflow)	0.000	7.000	0.000	0.7091	
	s(NO_3-N load)	0.000	7.000	0.000	0.7937	
	s(TP load)	0.000	7.000	0.000	0.7602	
	s(day)	2.583	3.000	4.372	0.0047	**
	s(ddate)	0.700	19.000	0.052	0.2401	

Signif. codes: 0 <= '***' < 0.001 < '**' < 0.01 < '*' < 0.05

Adjusted R-squared: 0.155, Deviance explained 0.285

-REML : 134.757, Scale est: 0.360, N: 46

Total Kjeldahl Nitrogen Model Summaries

Table 44. Temporal GAM summary for TKN concentration at TCEQ-13563.

Component	Term	Estimate	Std Error	t-value	p-value
A. parametric coefficients	(Intercept)	-0.072	0.051	-1.416	0.1637
Component	**Term**	**edf**	**Ref. df**	**F-value**	**p-value**
B. smooth terms	s(day)	1.391	3.000	0.932	0.1367
	s(ddate)	1.201	19.000	0.113	0.1684

Signif. codes: 0 <= '***' < 0.001 < '**' < 0.01 < '*' < 0.05

Adjusted R-squared: 0.0824, Deviance explained 0.149

-REML : 14.523, Scale est: 0.128, N: 49

Table 45. Inflow GAM summary for TKN concentration at TCEQ-13563.

Component	Term	Estimate	Std Error	t-value	p-value	
A. parametric coefficients	(Intercept)	-0.075	0.050	-1.520	0.1356	
Component	**Term**	**edf**	**Ref. df**	**F-value**	**p-value**	
B. smooth terms	s(inflow)	1.608	7.000	0.740	0.0398	*
	s(day)	1.060	3.000	0.556	0.2108	
	s(ddate)	0.000	19.000	0.000	0.5366	

Signif. codes: 0 <= '***' < 0.001 < '**' < 0.01 < '*' < 0.05

Adjusted R-squared: 0.125, Deviance explained 0.196

-REML : 13.279, Scale est: 0.121, N: 49

Table 46. Temporal GAM summary for TKN concentration at TCEQ-13383.

Component	Term	Estimate	Std Error	t-value	p-value	
A. parametric coefficients	(Intercept)	-0.085	0.063	-1.346	0.1856	
Component	**Term**	**edf**	**Ref. df**	**F-value**	**p-value**	
B. smooth terms	s(day)	0.000	3.000	0.000	0.5278	
	s(ddate)	2.203	19.000	0.491	0.0122	*

Signif. codes: 0 <= '***' < 0.001 < '**' < 0.01 < '*' < 0.05

Adjusted R-squared: 0.124, Deviance explained 0.223

-REML : 21.204, Scale est: 0.181, N: 45

Table 47. Inflow GAM summary for TKN concentration at TCEQ-13383.

Component	Term	Estimate	Std Error	t-value	p-value	
A. parametric coefficients	(Intercept)	-0.088	0.064	-1.374	0.1769	
Component	**Term**	**edf**	**Ref. df**	**F-value**	**p-value**	
B. smooth terms	s(inflow)	1.125	7.000	0.352	0.1150	
	s(day)	0.000	3.000	0.000	0.6250	
	s(ddate)	1.814	19.000	0.273	0.0544	.

Signif. codes: 0 <= '***' < 0.001 < '**' < 0.01 < '*' < 0.05

Adjusted R-squared: 0.154, Deviance explained 0.254

-REML : 20.749, Scale est: 0.187, N: 45

.

Table 48. Temporal GAM summary for TKN concentration at TCEQ-13384.

Component	**Term**	**Estimate**	**Std Error**	**t-value**	**p-value**	
A. parametric coefficients	(Intercept)	-0.287	0.073	-3.945	0.0003	***
Component	**Term**	**edf**	**Ref. df**	**F-value**	**p-value**	
B. smooth terms	s(day)	0.000	3.000	0.000	0.7689	
	s(ddate)	1.524	19.000	0.154	0.1485	

Signif. codes: 0 <= '***' < 0.001 < '**' < 0.01 < '*' < 0.05

Adjusted R-squared: 0.0426, Deviance explained 0.0938

-REML : 16.590, Scale est: 0.255, N: 48

Table 49. Inflow GAM summary for TKN concentration at TCEQ-13384.

Component	Term	Estimate	Std Error	t-value	p-value	
A. parametric coefficients	(Intercept)	-0.288	0.073	-3.962	0.0003	***
Component	**Term**	**edf**	**Ref. df**	**F-value**	**p-value**	
B. smooth terms	s(inflow)	0.200	7.000	0.027	0.3811	
	s(day)	0.000	3.000	0.000	0.7675	
	s(ddate)	1.497	19.000	0.148	0.1542	

Signif. codes: 0 <= '***' < 0.001 < '**' < 0.01 < '*' < 0.05

Adjusted R-squared: 0.0436, Deviance explained 0.0997

-REML : 16.583, Scale est: 0.254, N: 48

Dissolved Oxygen Model Summaries

Table 50. Temporal GAM summary for DO concentration at TCEQ-13563

Component	Term	Estimate	Std Error	t-value	p-value	
A. parametric coefficients	(Intercept)	2.060	0.014	152.339	0.0000	***
Component	**Term**	**edf**	**Ref. df**	**F-value**	**p-value**	
B. smooth terms	s(day)	2.663	3.000	29.706	0.0000	***
	s(ddate)	0.000	19.000	0.000	0.5000	

Signif. codes: 0 <= '***' < 0.001 < '**' < 0.01 < '*' < 0.05

Adjusted R-squared: 0.598, Deviance explained 0.647

-REML : 72.924, Scale est: 0.0102, N: 56

Table 51. Inflow GAM summary for DO concentration at TCEQ-13563

Component	Term	Estimate	Std Error	t-value	p-value	
A. parametric coefficients	(Intercept)	2.059	0.013	158.861	0.0000	***
Component	**Term**	**edf**	**Ref. df**	**F-value**	**p-value**	
B. smooth terms	s(inflow)	1.533	7.000	0.647	0.0522	.
	s(day)	2.692	3.000	31.795	0.0000	***
	s(ddate)	0.000	19.000	0.000	0.8661	

Signif. codes: 0 <= '***' < 0.001 < '**' < 0.01 < '*' < 0.05

Adjusted R-squared: 0.629, Deviance explained 0.686

-REML : 72.045, Scale est: 0.00941, N: 56

Table 52. Inflow plus load GAM summary for DO concentration at TCEQ-13563

Component	Term	Estimate	Std Error	t-value	p-value
A. parametric coefficients	(Intercept)	2.059	0.012	164.825	0.0000
Component	**Term**	**edf**	**Ref. df**	**F-value**	**p-value**
B. smooth terms	s(inflow)	1.762	7.000	1.012	0.0159
	s(NO_3-N load)	0.000	7.000	0.000	0.3201
	s(TP load)	1.419	7.000	0.412	0.1262
	s(day)	2.695	3.000	33.467	0.0000
	s(ddate)	0.000	19.000	0.000	0.8755

Signif. codes: 0 <= '***' < 0.001 < '**' < 0.01 < '*' < 0.05

Adjusted R-squared: 0.648, Deviance explained 0.716

-REML : 71.850, Scale est: 0.00874, N: 56

Table 53. Temporal GAM summary for DO concentration at TCEQ-13383

Component	**Term**	**Estimate**	**Std Error**	**t-value**	**p-value**	
A. parametric coefficients	(Intercept)	1.966	0.016	123.304	0.0000	***
Component	**Term**	**edf**	**Ref. df**	**F-value**	**p-value**	
B. smooth terms	s(day)	2.493	3.000	24.979	0.0000	***
	s(ddate)	0.285	19.000	0.021	0.2411	

Signif. codes: 0 <= '***' < 0.001 < '**' < 0.01 < '*' < 0.05

Adjusted R-squared: 0.547, Deviance explained 0.600

-REML : 75.725, Scale est: 0.014, N: 55

Table 54. Inflow GAM summary for DO concentration at TCEQ-13383

Component	Term	Estimate	Std Error	t-value	p-value	
A. parametric coefficients	(Intercept)	1.966	0.016	123.304	0.0000	***
Component	**Term**	**edf**	**Ref. df**	**F-value**	**p-value**	
B. smooth terms	s(inflow)	0.000	7.000	0.000	0.8622	
	s(day)	2.493	3.000	24.979	0.0000	***
	s(ddate)	0.285	19.000	0.021	0.2410	

Signif. codes: 0 <= '***' < 0.001 < '**' < 0.01 < '*' < 0.05

Adjusted R-squared: 0.547, Deviance explained 0.600

-REML : 75.725, Scale est: 0.014, N: 55

Table 55. Inflow plus load GAM summary for DO concentration at TCEQ-13383

Component	Term	Estimate	Std Error	t-value	p-value
A. parametric coefficients	(Intercept)	1.966	0.016	125.358	0.0000
Component	**Term**	**edf**	**Ref. df**	**F-value**	**p-value**
B. smooth terms	s(inflow)	0.000	7.000	0.000	0.8008
	s(NO_3-N load)	0.859	7.000	0.274	0.1102
	s(TP load)	0.000	7.000	0.000	0.8822
	s(day)	2.504	3.000	26.573	0.0000
	s(ddate)	0.106	19.000	0.006	0.2889

Signif. codes: 0 <= '***' < 0.001 < '**' < 0.01 < '*' < 0.05

Adjusted R-squared: 0.560, Deviance explained 0.618

-REML : 75.399, Scale est: 0.0135, N: 55

Table 56. Temporal GAM summary for DO concentration at TCEQ-13384.

Component	**Term**	**Estimate**	**Std Error**	**t-value**	**p-value**	
A. parametric coefficients	(Intercept)	2.007	0.015	138.110	0.0000	***
Component	**Term**	**edf**	**Ref. df**	**F-value**	**p-value**	
B. smooth terms	s(day)	2.591	3.000	30.673	0.0000	***
	s(ddate)	0.535	19.000	0.044	0.2107	

Signif. codes: 0 <= '***' < 0.001 < '**' < 0.01 < '*' < 0.05

Adjusted R-squared: 0.611, Deviance explained 0.658

-REML : 70.737, Scale est: 0.0114, N: 54

Table 57. Inflow GAM summary for DO concentration at TCEQ-13384.

Component	Term	Estimate	Std Error	t-value	p-value	
A. parametric coefficients	(Intercept)	2.006	0.014	140.003	0.0000	***
Component	**Term**	**edf**	**Ref. df**	**F-value**	**p-value**	
B. smooth terms	s(inflow)	0.558	7.000	0.119	0.2206	
	s(day)	2.592	3.000	31.377	0.0000	***
	s(ddate)	0.652	19.000	0.061	0.1725	

Signif. codes: 0 <= '***' < 0.001 < '**' < 0.01 < '*' < 0.05

Adjusted R-squared: 0.621, Deviance explained 0.669

-REML : 70.662, Scale est: 0.0111, N: 54

Table 58. Inflow plus load GAM summary for DO concentration at TCEQ-13384.

Component	Term	Estimate	Std Error	t-value	p-value
A. parametric coefficients	(Intercept)	2.006	0.014	140.003	0.0000
Component	**Term**	**edf**	**Ref. df**	**F-value**	**p-value**
B. smooth terms	s(inflow)	0.558	7.000	0.118	0.2206
	s(NO_3-N load)	0.000	7.000	0.000	0.5777
	s(TP load)	0.000	7.000	0.000	0.3485
	s(day)	2.592	3.000	31.376	0.0000
	s(ddate)	0.652	19.000	0.061	0.1726

Signif. codes: 0 <= '***' < 0.001 < '**' < 0.01 < '*' < 0.05

Adjusted R-squared: 0.621, Deviance explained 0.669

-REML : 70.662, Scale est: 0.0111, N: 54